TABLE 2. Characteristics of Patients with UC in a Caucasian Cohort

Characteristics	Patients with UC
Number (male:female)	30 (18:12)
Age, yr, mean (SD)	42.9 (17.9)
Age at diagnosis, yr, mean (SD)	33.2 (15.7)
Treatment	
Salazosulfapyridine or mesalazine, *N* (%)	14 (46.7)
Steroids, *N* (%)	9 (30.0)
Immunomodulators, *N* (%)	11 (36.7)
Anti-TNF therapy	3 (10.0)
Disease location (*N*)	
Extensive colitis/left-sided colitis/proctitis	16/11/3

in duplicate. The intraassay coefficients of variations for human LRG and mouse LRG were ≤7.98% and ≤8.93%, respectively. For the quantification of IL-6, TNF-α, and IL-22 in human serum samples, the human IL-6 Ultra Sensitive ELISA (Biosource International, Camarillo, CA), human TNF-α UltraSensitive ELISA kit (Invitrogen, Carlsbad, CA), and human IL-22 Quantikine ELISA Kit (R&D Systems, Minneapolis, MN) were used following the manufacturer's guidelines.

Western Blot Analysis

Frozen colon tissue samples were lysed in RIPA buffer (10 mM Tris-HCl, pH 7.5, 150 mM NaCl, 1% Nonidet P-40, 0.1% sodium deoxycholate, 0.1% SDS, 1 × protease inhibitor cocktail; Nacalai Tesque, Kyoto, Japan) and 1 × phosphatase inhibitor cocktail (Nacalai Tesque) followed by centrifugation (13,200 rpm, 4°C, 15 minutes), after which the supernatants were stored at −80°C until use. Extracted proteins were subjected to sodium dodecyl sulfate-polyacrylamide gel electrophoresis (SDS-PAGE) as described previously.[21] Samples transferred onto PVDF membranes were treated with a rabbit antihuman LRG polyclonal antibody (Proteintech Group, Chicago, IL) or a rabbit anti-GAPDH polyclonal antibody (Santa Cruz Biotechnology, Santa Cruz, CA) was used as described previously.[21]

Immunohistochemistry

Immunohistochemical analyses were performed according to a method described in our previous report.[22] Briefly, rabbit antihuman LRG polyclonal antibodies were used as the primary antibody. After incubation with the primary antibodies, the sections were treated with biotin-conjugated goat anti-rabbit IgG (Vector Laboratories, Burlingame, CA) and avidin-biotin-peroxidase complexes (Vector Laboratories). Immunoreactive cells were visualized with a diaminobenzidine substrate (Merck, Darmstadt, Germany) and were counterstained with hematoxylin.

Mice

C57BL/6 mice were purchased from Clea Japan (Tokyo, Japan). C57BL/6-background IL-6-deficient mice were kindly provided by Professor Yoichiro Iwakura (Laboratory of Molecular Pathogenesis, Center for Experimental Medicine, Institute of Medical Science, University of Tokyo, Tokyo, Japan). Mice were maintained under specific pathogen-free conditions. C57BL/6 and IL-6-deficient mice were used at 7–9 weeks of age. All experiments were conducted according to the institutional ethical guidelines for animal experimentation.

LPS-mediated Acute Inflammation

To induce acute inflammation, wildtype (WT) mice and IL-6-deficient mice were injected intraperitoneally with 0 or 10 mg/kg LPS (*Escherichia coli* LPS, Sigma, St. Louis, MO) dissolved in 500 μL phosphate-buffered saline (PBS). Blood was collected at before and 24 hours after LPS injection and the serum was separated by centrifugation and stored at −30°C until used for ELISA analysis.

Induction of Colitis

For induction of colitis, WT mice and IL-6-deficient mice were given 3% dextran sodium sulfate (DSS) (m/w 36,000–50,000; MP Biomedicals, Solon, OH) dissolved in drinking water provided ad libitum for 5 days, followed by provision of ordinary water for 20 days.

Assessment of Severity of DSS-induced Colitis

WT mice were weighed daily from day 0 to day 25. Changes in body weight were calculated as follows: body weight change (%) = [(weight on a given day (days 0–13) − weight on day 0)/weight on day 0] * 100. Blood was collected from WT mice on days 5, 7, 10, 15, and 25 after DSS administration or day 0 by cardiac puncture under anesthesia and on days 0 and 10 from IL-6-deficient mice. The serum was separated by centrifugation and stored at −30°C until used for ELISA analysis.

Cell Culture

The human colonic adenocarcinoma COLO205 cell line was obtained from the American Type Culture Collection (ATCC, Manassas, VA). Cells were maintained in RPMI 1640 medium supplemented with 10% fetal bovine serum (FBS) (HyClone Laboratories, Logan, UT) and 1% penicillin–streptomycin (Nacalai Tesque) at 37°C under a humidified atmosphere of 5% CO_2.

For the analysis of LRG protein induction, COLO205 cells were stimulated with various concentrations of cytokines for 24 hours and culture supernatant were concentrated using Amicon Ultra-4 10K MWCO (Millipore, Bedford, MA). Concentrated supernatants were used for western blot analysis. Full-length human LRG cDNA was inserted into pcDNA3.1/V5-His-TOPO vector (Invitrogen) and designated pcDNA3.1-LRG-V5-His. pcDNA3.1-LRG-V5-His vector was transfected

into COS7 cells using Lipofectamine 2000 reagent (Invitrogen) and culture medium were used for the positive control.

Quantitative Real-time Reverse-transcription Polymerase Chain Reaction (RT-PCR) Analysis

For the quantification of mRNA levels of LRG, various mouse organs were analyzed by real-time RT-PCR as described previously.[23] Levels of mouse LRG and mouse hypoxanthine phosphoribosyltransferase (HPRT) levels were determined by the 7900HT Real-time PCR system (Applied Biosystems, Foster City, CA) using specific primers: murine LRG forward 5′-ATCAAGGAAGCCTCCAGGAT-3′; reverse 5′-CAGCTGCGTCAGGTTGG-3′ and murine hypoxanitine phosphoribosyltransferase (HPRT) forward 5′-TCAGTCAACG GGGGACATAAA-3′; reverse 5′-GGGGCTGTACTGCTT AACCAG-3′.

Statistics

The Mann–Whitney *U*-test or one-way analysis of variance (ANOVA) followed by a Scheffe's test were used for statistical analyses. Two-tailed Student's *t*-test was used for significant differences in LRG expression between identical patients with UC in active and remission disease stage. One-way ANOVA followed by a Dunnett's test was used for multiple comparison of the difference of serum LRG levels at various timepoints after DSS treatment in mice. Pearson's test was used to analyze the relationship between LRG and CRP, IL-6, or CAI. For drawing of receiver operating characteristic (ROC) curves and estimation of the area under the ROC curve (AUC) statistics, the software Excel Statistics 2010 (Social Survey Research Information, Tokyo, Japan) was used to quantify the ability to differentiate between remission and active by CAI. $P < 0.05$ was considered significant.

Ethical Considerations

Informed consent was obtained from all donors and all studies involving human subjects were approved by the Institutional Review Boards of the National Institute of Biomedical Innovation, Osaka University Hospital, the Department of Surgery, Osaka Rosai Hospital, and the University of North Carolina.

RESULTS

Serum LRG Levels Are Increased in Active UC Patients

We quantified serum LRG concentrations by ELISA using sera from patients with UC. Serum LRG concentrations were significantly elevated in the active UC patients (CAI ≥6) (14.24 ± 8.08 μg/mL) compared with HC (3.07 ± 1.42 μg/mL; $P < 0.0001$) (Fig. 1A). There was also a significant difference between LRG serum levels in patients with active UC (CAI ≥6) (14.24 ± 8.08 μg/mL) compared with UC in remission (CAI <6) (5.34 ± 2.60 μg/mL; $P <$ 0.0001) (Fig. 1A). To determine whether serum LRG levels are increased in non-IBD disease controls, we quantified serum LRG levels in patients with appendicitis and

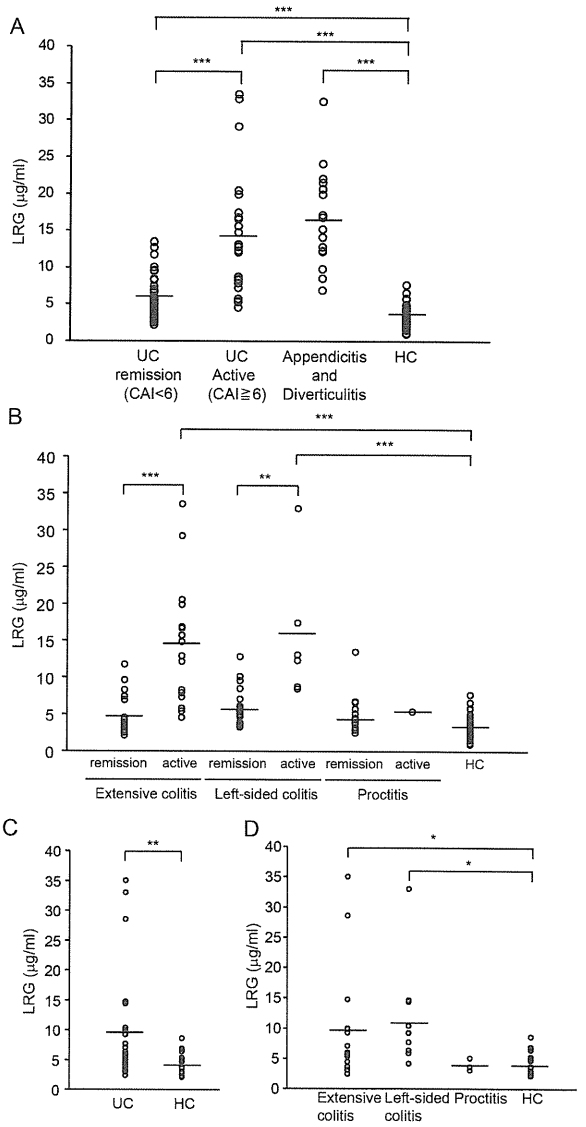

FIGURE 1. Serum LRG levels are increased in patients with active UC. (A) Serum levels of LRG were determined in 82 patients with UC (57 patients in remission [CAI <6], 25 patients in active [CAI ≥6] stage), appendicitis ($n = 13$), diverticulitis ($n = 4$) and 50 healthy controls (HC). ***$P < 0.0001$ by one-way ANOVA followed by Scheffe's post-hoc test. (B) Disease extension in UC was grouped into three categories: In UC patients in remission, extensive colitis ($n = 19$), left-sided colitis ($n = 24$), and proctitis ($n = 14$); in active patients, extensive colitis ($n = 18$), left-sided colitis ($n = 6$), and proctitis ($n = 1$) and HC ($n = 50$). **$P < 0.005$, ***$P < 0.0001$ by one-way ANOVA followed by Scheffe's post-hoc test. (C) Serum levels of LRG were determined in patients with UC ($n = 30$) and HC ($n = 19$) in a Caucasian cohort. **$P < 0.005$ by Mann–Whitney *U*-test. (D) In a Caucasian cohort, disease extension in UC was grouped into three categories: extensive colitis ($n = 16$), left-sided colitis ($n = 11$), and proctitis ($n = 3$) and HC ($n = 19$). *$P < 0.05$ by one-way ANOVA followed by Scheffe's post-hoc test.

diverticulitis. Elevated serum LRG levels were also observed in appendicitis and diverticulitis (16.83 ± 6.50 μg/mL) compared with HC (3.07 ± 1.42 μg/mL; $P < 0.0001$) (Fig. 1A), suggesting that serum LRG levels are also increased in acute intestinal inflammation.

When UC were classified into three categories based on disease extent, significantly higher serum LRG concentrations were observed in active patients with extensive colitis (14.34 ± 7.89 μg/mL) compared with in remission (4.96 ± 2.68 μg/mL; $P < 0.0001$) and HC (3.07 ±1.42 μg/mL; $P < 0.0001$) and active patients with left-sided colitis (15.41 ± 9.16 μg/mL) compared with in remission (5.91 ± 2.41 μg/mL; $P = 0.0003$) and HC (3.07 ±1.42 μg/mL; $P = 0.001$) (Fig. 1B). Nonetheless, there was no clear difference between active patients with proctitis and HC, possibly due to the low number of patients in this group. In patients with UC in remission, serum LRG levels in all of three disease extent categories were comparable with HC (Fig. 1B). Significantly elevated serum LRG levels were also detected in a Caucasian UC cohort (9.46 ± 8.44 μg/mL) compared with HC (4.42 ± 1.91 μg/mL; $P < 0.005$) (Fig. 1C). In this Caucasian UC cohort, serum LRG levels were also significantly elevated in patients with extensive colitis (9.54 ± 8.05 μg/mL) compared with HC (4.42 ± 1.91 μg/mL; $P < 0.05$) and left-sided colitis (10.90 ± 9.16 μg/mL) compared with HC (4.42 ± 1.91 μg/mL; $P < 0.02$) (Fig. 1D). However, a clear difference was not observed between patients with proctitis and HC (Fig. 1D). These results suggest that serum LRG levels were elevated in active UC.

Serum LRG Levels Are Correlated with Disease Activity in UC Patients

We investigated the correlation between serum LRG levels and disease activity (CAI) in UC patients. A positive correlation was observed between LRG and CAI ($r = 0.731$, $P < 0.00001$) (Fig. 2A). This correlation was stronger than that observed between CRP and CAI ($r = 0.654$, $P < 0.00001$) (Fig. 2A). When patients with UC were classified into active and remission according to the endoscopic findings, significantly elevated serum LRG levels and CRP levels were observed in patients with active UC compared with patients in remission ($P < 0.005$, respectively) (Supporting Fig. 1A). While serum LRG levels were significantly correlated with CRP levels in patients with UC ($r = 0.850$, $P < 0.00001$, $n = 82$) (Supporting Fig. 2A), such a correlation was not found when a CRP-negative subgroup (CRP <0.2, $n = 51$) was analyzed ($r = 0.101$, $P = 0.481$) (Supporting Fig. 2B). In this CRP-negative group, serum LRG levels were significantly correlated with CAI ($r = 0.416$, $P = 0.00241$) (Supporting Fig. 2C); however, significant correlation was not found between CRP and CAI ($r = -0.0896$, $P = 0.532$) (Supporting Fig. 2D). Additionally, in the CRP-negative group elevated serum LRG levels were detected in patients with endoscopically active UC compared with patients with UC in remission ($P = 0.0442$) (Supporting Fig. 1B). These findings in patients with low CRP may explain a better correlation of CAI with LRG than that with CRP.

When UC was classified by disease extent, a significantly higher positive correlation was detected between LRG and CAI than CRP and CAI both in extensive colitis ($r = 0.690$, $P < 0.000001$ and $r = 0.580$, $P = 0.000168$) and left-sided colitis ($r = 0.840$, $P < 0.000001$ and $r = 0.759$, $P < 0.000001$), but not in proctitis (Fig. 2B). Importantly, by analyzing sera obtained at active (CAI ≥6) and remission (CAI <6) disease stages from 10 identical UC patients, a significant decrease in serum LRG levels in remission was detected (Fig. 2C).

By generating an ROC curve, the sensitivity and specificity of serum LRG for remission and active by CAI were determined (Fig. 2D). The AUC for serum LRG levels was 0.901, whereas the AUC for CRP levels was 0.845. The cutoff value of serum LRG levels was 7.21 μg/mL (sensitivity = 84.0%, specificity = 82.5%). In contrast, when the cutoff value of CRP levels was set to 0.20, a maximum CRP value of normal range, the sensitivity was 80.0% and the specificity was 80.7%. These results emphasize the usefulness of monitoring serum LRG levels for the evaluation of the disease activity of UC.

Expression of LRG Was Increased in Inflamed UC Colons

Next, to investigate whether local inflammatory sites in patients with UC are a potential source of increased serum LRG we first looked at the expression of LRG in the colon by western blot analysis on inflamed and noninflamed sites of surgically resected full-thickness colon specimens from patients with UC. Western blot analysis showed that LRG expression in colon tissues was increased in inflamed sites of active UC patients compared with noninflamed colon tissues (Fig. 3A). Next, we tried to examine the localization of LRG. By immunohistochemistry, increased expression of LRG was detected in the cytoplasm of intestinal epithelial cells (IECs) in inflamed tissues (Fig. 3B–E). In contrast, expression of LRG was lower in noninflamed tissues (Fig. 3B–E). These data suggest that inflamed colon tissue is a potential source of increased serum LRG in patients with UC.

LRG Is Induced by Stimulation with TNF-α, IL-6, or IL-22

It has been reported that IL-6 is an inducer of LRG expression.[16] However, it is not clear whether LRG is induced by cytokines other than IL-6. At first we investigated the serum levels of IL-6, IL-22, and TNF-α, known

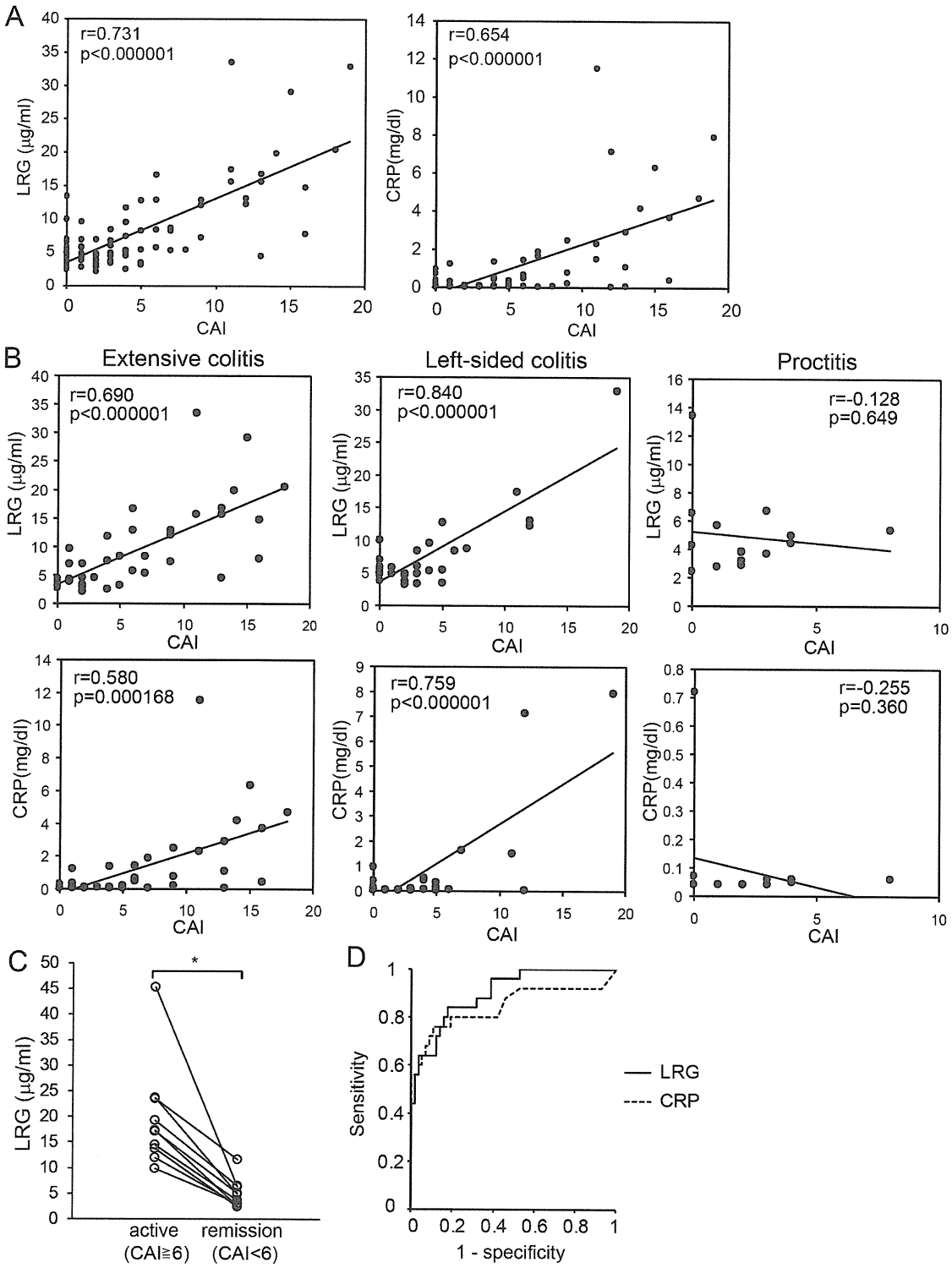

FIGURE 2. Serum LRG levels are correlated with disease activity better than CRP in patients with UC. (A) Serum levels of LRG correlated with CAI ($n = 82$; $P < 0.000001$; $r = 0.731$) better than CRP ($n = 82$; $P < 0.000001$; $r = 0.654$) in patients with UC. (B) Serum levels of LRG correlated with disease activity in extensive colitis ($n = 37$; $P < 0.000001$; $r = 0.690$) and left-sided colitis ($n = 30$; $P < 0.000001$; $r = 0.840$) better than CRP in extensive colitis ($n = 37$; $P = 0.000168$; $r = 0.580$) and left-sided colitis ($n = 30$; $P < 0.000001$; $r = 0.759$), while neither LRG ($n = 15$; $P = 0.649$; $r = -0.128$) nor CRP levels ($n = 15$; $P = 0.360$; $r = -0.255$) were correlated with disease activity in proctitis. (C) Compared with 10 identical active patients with UC, serum levels of LRG were decreased in remission. *$P < 0.002$ by Student's t-test. (D) ROC curves for LRG and CRP for differentiation between UC patients with remission ($n = 57$) and active ($n = 25$) by CAI.

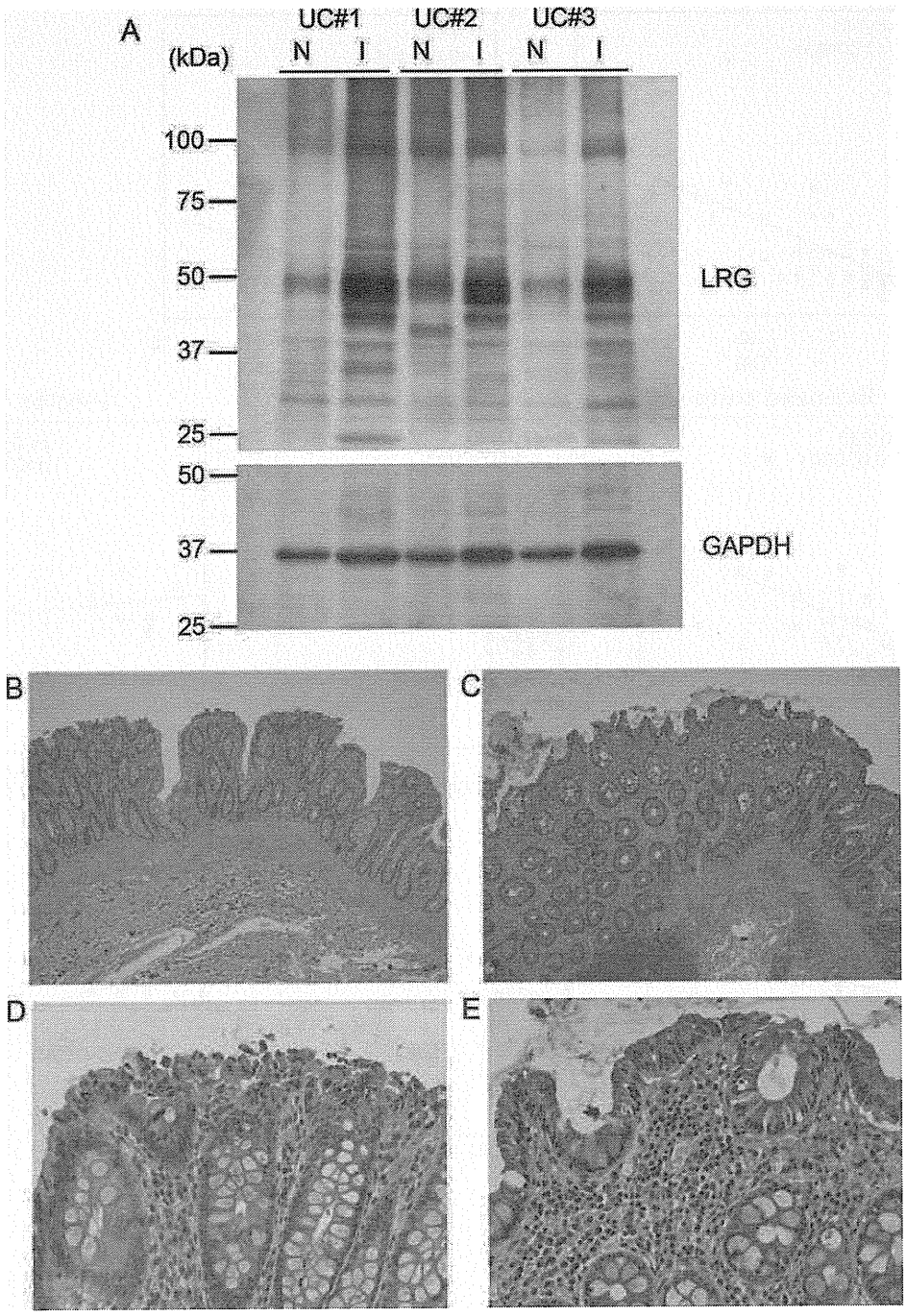

FIGURE 3. Expression of LRG is increased in lesion sites of ulcerative colitis. (A) Representative western blot analysis of three separate experiments for LRG using paired surgically resected full-thickness colon specimens from noninflamed (N) and inflamed (I) sites in patients with UC. GAPDH was used as a control of the relative amounts of proteins in each sample. Full-thickness colon tissues from UC in inflamed and noninflamed sites were evaluated by immunohistochemical analysis for LRG expression ($n = 10$ per experimental group). (B) Noninflamed mucosa (×42). (C) Inflamed mucosa from active UC (×42). (D) Noninflamed mucosa (×400). (E) Inflamed mucosa from active UC (×400).

to be increased at the inflamed tissue in active UC.[24–26] Indeed, ELISA analysis using sera from 82 UC patients revealed that serum TNF-α, IL-6, and IL-22 levels were significantly elevated in active UC patients compared with those patients in remission ($P = 0.0178$, $P = 0.00690$, and $P < 0.0001$, respectively) (Fig. 4A). Next, to investigate

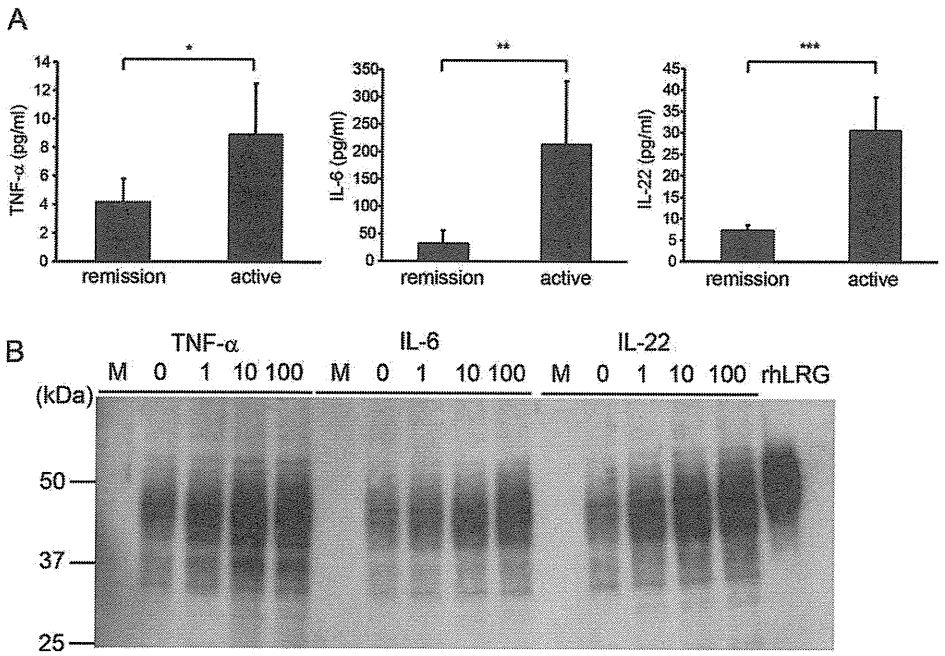

FIGURE 4. Expression of LRG was induced by TNF-α, IL-6, and IL-22. (A) Serum levels of TNF-α, IL-6, and IL-22 were determined in patients with UC (57 patients in remission [CAI <6] and 25 patients in active [CAI ≥6] stage). Data are expressed as mean ± SEM. *$P < 0.05$, **$P < 0.005$, ***$P < 0.0001$ by Mann–Whitney U-test. (B) LRG was determined in supernatants of COLO205 cells left untreated or stimulated with TNF-α, IL-6, and IL-22 at 1.0, 10, 100 ng/mL for 24 hours and analyzed by western blotting. There was a dose-dependent increase in LRG levels after treatment with TNF-α, IL-6, and IL-22.

which proinflammatory cytokines induce expression of LRG we stimulated human colonic adenocarcinoma COLO205 cells with TNF-α, IL-6, or IL-22 for 24 hours. After cytokine stimulation, secretion of LRG protein into the culture media was analyzed by western blotting. Interestingly, LRG was induced not only by stimulation with IL-6, but also by TNF-α and IL-22 in a dose-dependent manner (Fig. 4B). These results indicate that expression of LRG is induced by various proinflammatory cytokines including IL-6.

Expression of LRG Through an IL-6-independent Pathway Is Demonstrated in LPS-mediated Acute Inflammation and DSS-induced Colitis

CRP is one of the representative acute phase proteins in humans and CRP production is primarily dependent on liver by circulating IL-6. To examine the possible differences in induction mechanisms between LRG and CRP, particularly with regard to the involvement of IL-6, we took advantage of murine models. We first assessed whether LRG is induced in WT mice by injecting LPS, an inducer of proinflammatory cytokines from macrophages, because CRP is poorly induced in mice during acute inflammation. At 24 hours after intraperitoneal injection of LPS, serum samples were prepared and serum LRG levels were determined by ELISA. Compared with WT mice, significant elevation of serum LRG levels were detected in LPS-administered WT mice (Fig. 5A), suggesting that LRG is induced during acute inflammation in mice as in humans.

We next used a murine IBD model to investigate induction mechanisms of LRG during colonic inflammation. DSS-induced colitis is often used as a murine model of UC.[27] We induced colitis in WT mice by treating them with 3% DSS for 5 days and measured changes in relative body weight. Body weight began to decrease at day 5, showed greatest reduction at day 9, and recovered at 18 days after DSS treatment (Fig. 5B). We analyzed changes in serum LRG levels by ELISA before and 5, 7, 10, 15, and 25 days after DSS treatment. Consistent with body weight loss, serum LRG levels were significantly elevated at 5 days after DSS treatment (Fig. 5C). Serum LRG levels remained high until day 15, but decreased at day 25. Delayed normalization of serum LRG levels is likely due to the prolonged inflammation at inflamed tissue sites. Additionally, a long half-life of serum LRG might also be involved in this, since our preliminary data suggest that the half-life of serum human LRG levels are about two times longer than that of CRP (data not shown). To investigate which organs produce LRG in DSS-induced colitis, RNA was extracted from colon, liver, and spleen before and 9 days after DSS treatment. By quantitative PCR analysis (Fig. 5D), expression of LRG was significantly increased in liver ($P = 0.00106$) and spleen ($P = 0.0376$);

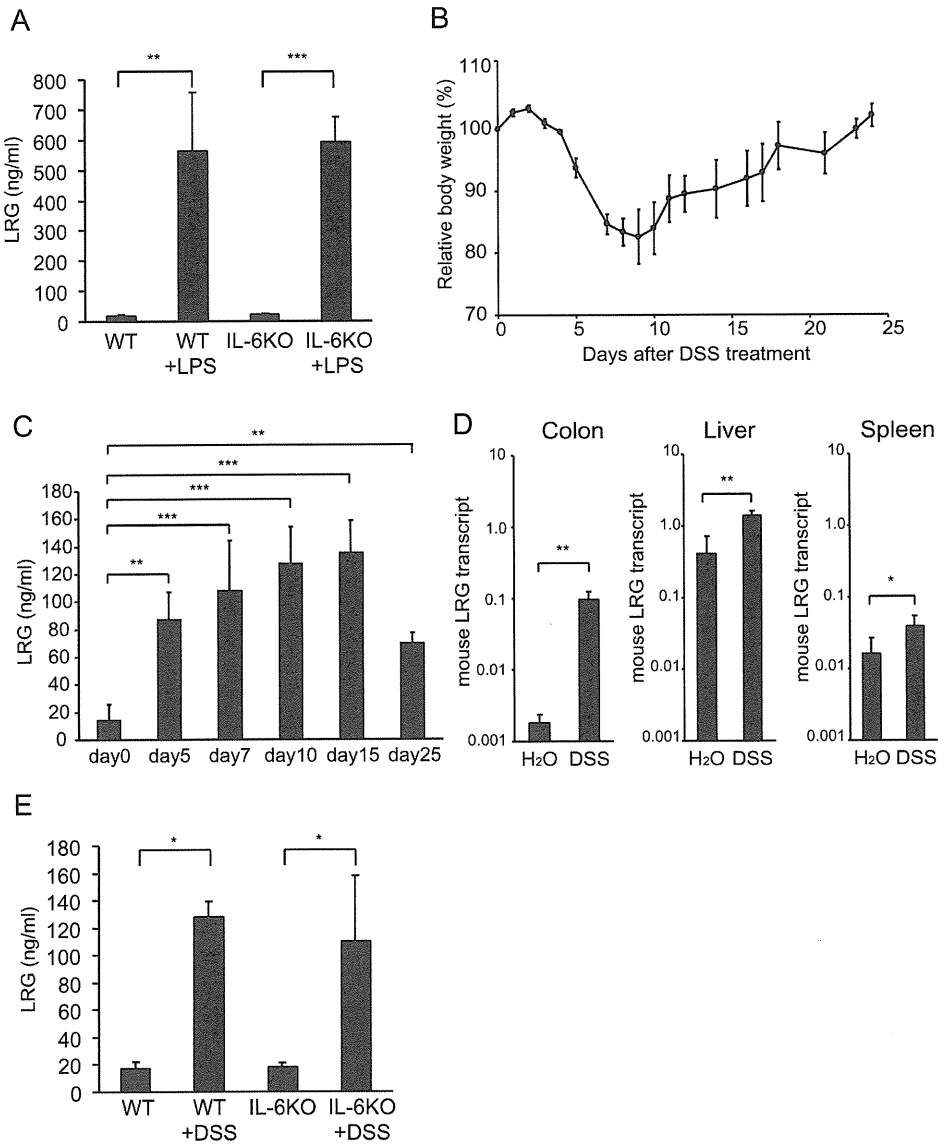

FIGURE 5. Induction of LRG has IL-6-independent pathway in LPS-mediated acute inflammation and active stage of DSS-induced colitis. (A) WT mice and IL-6-deficient mice were injected intraperitoneally with 0 or 10 mg/kg LPS dissolved in 500 μL PBS and serum LRG levels were measured after 24 hours. Data are expressed as mean ± SEM. $^{**}P < 0.005$, $^{***}P < 0.0001$ by one-way ANOVA followed by Scheffe's post-hoc test. (B) Relative body weight changes of mice with DSS-induced colitis in this study. Data are expressed as mean ± SEM ($n = 4$). (C) Expression of LRG is upregulated in murine DSS-induced colitis. At the indicated time, serum LRG levels were determined by ELISA analysis. $^{**}P < 0.005$, $^{***}P < 0.0001$ by one-way ANOVA followed by a by Dunnett's post-hoc test. (D) Nine days after control or DSS treatment, mice were euthanized and gene expression of LRG in the colon, liver, spleen, and kidney was determined by quantitative PCR analysis. Gene expression was calculated relative to HPRT. Data were expressed as mean ± SD ($n = 5$). $^{*}P < 0.05$, $^{**}P < 0.005$ by Student's t-test. (E) IL-6-deficient mice were used for DSS-induced colitis. Nine days after DSS administration, serum levels of mouse LRG was determined by ELISA analysis. $^{*}P < 0.05$ by one-way ANOVA followed by Scheffe's post-hoc test.

however, the strongest induction was observed in colon ($P = 0.000126$).

To investigate whether LRG induction is dependent on IL-6 or not, we analyzed serum LRG levels in IL-6-deficient mice. Interestingly, basal LRG levels in IL-6-deficient mice were similar to those in WT mice and LRG was robustly induced by LPS administration in IL-6-deficient mice (Fig. 5A). Moreover, increased serum LRG levels were also detected in the active stage (day 9) of DSS-induced colitis in IL-6-deficient mice (Fig. 5E). Importantly, the increase of serum LRG in IL-6-deficient mice was similar to that in WT mice (Fig. 5A,E). These findings indicate that LRG expression can be induced in the absence of IL-6.

DISCUSSION

In this study we first demonstrated that serum LRG levels were significantly increased in sera of active UC patients compared with patients in remission and HC. Serum LRG is likely elevated in diverse racial groups, because we detected increased serum LRG levels not only in Japanese patients (Fig. 1A)[13] but also in Caucasian patients with UC (Fig. 1C,D) and CD (data not shown). In addition, levels of serum LRG were significantly correlated with disease activity in UC and the correlation was stronger than CRP. Moreover, by analyzing ROC curve and AUC, serum LRG levels showed higher AUC than CRP and serum LRG levels represented superior sensitivity and specificity to CRP for remission and active of UC by CAI (Fig. 2D), indicating that LRG is a useful marker to evaluate disease activity in UC. In the normal state, serum LRG is thought to be produced from liver and LRG is abundantly found in the sera of HC. In colonic inflammation, we found that the expression of LRG is increased in the inflamed mucosa of UC patients and mice with DSS colitis, suggesting that inflamed tissues can be a source for production of LRG (Fig. 3). The increased expression of LRG in inflamed tissue has previously been observed in appendix during acute appendicitis.[28] Moreover, in acute inflammatory disorders, including appendicitis and diverticulitis, increased expression of serum LRG was observed (Fig. 1A). These results indicate that the elevated expression of LRG at inflamed sites and in sera occurs in various acute and chronic inflammatory disorders. Therefore, increased serum LRG levels are not suitable for use as a specific diagnostic marker of IBD.

CRP is the most common serum marker used to evaluate disease activity in inflammatory diseases. However, serum CRP is primarily dependent on liver production induced by circulating IL-6. Compared with CD and RA, only modest to absent CRP responses are observed in UC, despite active inflammation in colon.[9] Indeed, our cohort of 82 UC patients, analyzed in this study, included five patients with normal value of CRP while having active disease (Fig. 2A). However, our study demonstrated that serum LRG levels were significantly increased in active UC patients' sera and correlated better with disease activity of UC than CRP levels (Figs. 1A, 2A). Particularly, in the group of patients with negative CRP (CRP <0.2), significant correlation was observed between serum LRG levels and CAI (Supporting Fig. 2C). Similarly, among CRP-negative patients serum LRG levels were significantly elevated in those with endoscopically active UC, compared with UC in remission (Supporting Fig. 1B). In addition, serum LRG levels were decreased after therapy (Fig. 2C), suggesting that LRG is a useful serological biomarker for evaluating disease activity and therapeutic effect in UC.

Better correlation of serum LRG levels with disease activity of UC than CRP might be explained in part by the differences in induction mechanisms between LRG and CRP. While the expression of CRP is essentially dependent on IL-6, several cytokines may compensate for the absence of elevated IL-6 in induction of LRG expression. Accordingly, expression of LRG in COLO205 cells was induced not only by IL-6 but also by TNF-α and IL-22 (Fig. 4B), all of which were increased in sera of UC patients (Fig. 4A). Expression of LRG was strongly induced by IL-22 in COLO205 cells, correlating with enhanced STAT3 (Tyr705) phosphorylation by IL-22 compared with IL-6 (data not shown). Thus, inflammatory cytokines such as TNF-α and IL-22 may mediate LRG expression in the absence of IL-6. Moreover, using DSS-induced colitis in IL-6-deficient mice we could demonstrate an IL-6-independent pathway for LRG induction (Fig. 5E). Because promoter regions of human and mouse LRG share high sequence homology and contain putative binding sites for transcription factors such as C/EBP, MZF1, and STAT,[17] it is conceivable that the similar IL-6-independent mechanisms of LRG induction are also involved in humans. Future studies are required to fully elucidate the induction mechanisms of LRG in both humans and mice.

In the three disease categories of UC based on extent of disease, serum LRG levels tended to be low in proctitis compared with extensive colitis and left-sided colitis (Fig. 1B). In addition, correlation between serum LRG levels and disease activity did not reach significance in proctitis (Fig. 2B). Although the low number of patients with active proctitis may preclude the proper evaluation of LRG levels, limited inflamed area of proctitis may also be a reason for slight increases of serum LRG levels in these patients. Given the increased production of LRG in inflamed colonic mucosa, fecal LRG might be a more sensitive disease biomarker for UC including proctitis. Optimization for the measurement of fecal LRG is currently under way in our laboratory.

This study also highlights the potential usefulness of LRG in evaluating murine colitis. Our results indicate that serum LRG levels increase as the disease progresses in a DSS-induced colitis model (Fig. 5B,C). In addition, the LRG expression is significantly upregulated in the colon with DSS-induced colitis (Fig. 5D). Thus, LRG in mice can be an objective disease activity marker for colitis models and may be useful for preclinical studies of IBD.

In conclusion, serum LRG levels reflect disease activity of UC better than CRP, especially in patients with low CRP. In the inflammatory condition, LRG is expressed in the inflamed tissue and expression of LRG is regulated by mechanisms different from that of CRP. These findings suggest that serum LRG is a novel and potential serologic biomarker for evaluating disease activity of UC.

ACKNOWLEDGMENTS

We thank T. Mizushima for provision of appendicitis and diverticulitis patients' sera, Y. Kanazawa for secretarial

assistance, and M. Urase and A. Morimoto for technical assistance.

REFERENCES

1. Nikolaus S, Schreiber S. Diagnostics of inflammatory bowel disease. *Gastroenterology*. 2007;133:1670–1689.
2. Baumgart DC, Sandborn WJ. Inflammatory bowel disease: clinical aspects and established and evolving therapies. *Lancet*. 2007;369: 1641–1657.
3. Stange EF, Travis SP, Vermeire S, et al. European evidence based consensus on the diagnosis and management of Crohn's disease: definitions and diagnosis. *Gut*. 2006;55(Suppl 1):i1–15.
4. Caprilli R, Viscido A, Latella G. Current management of severe ulcerative colitis. *Nat Clin Pract Gastroenterol Hepatol*. 2007;4:92–101.
5. Kornbluth A, Sachar DB. Ulcerative colitis practice guidelines in adults (update): American College of Gastroenterology, Practice Parameters Committee. *Am J Gastroenterol*. 2004;99:1371–1385.
6. Sands BE, Abreu MT, Ferry GD, et al. Design issues and outcomes in IBD clinical trials. *Inflamm Bowel Dis*. 2005;11(Suppl 1):S22–28.
7. Freeman HJ. Use of the Crohn's disease activity index in clinical trials of biological agents. *World J Gastroenterol*. 2008;14:4127–4130.
8. Best WR, Becktel JM, Singleton JW, et al. Development of a Crohn's disease activity index. National Cooperative Crohn's Disease Study. *Gastroenterology*. 1976;70:439–444.
9. Vermeire S, Van Assche G, Rutgeerts P. C-reactive protein as a marker for inflammatory bowel disease. *Inflamm Bowel Dis*. 2004;10: 661–665.
10. Pepys MB, Druguet M, Klass HJ, et al. Immunological studies in inflammatory bowel disease. *Ciba Found Symp* 1977:283–304.
11. Saverymuttu SH, Hodgson HJ, Chadwick VS, et al. Differing acute phase responses in Crohn's disease and ulcerative colitis. *Gut*. 1986; 27:809–813.
12. Colombel JF, Rutgeerts P, Reinisch W, et al. Early mucosal healing with infliximab is associated with improved long-term clinical outcomes in ulcerative colitis. *Gastroenterology*. 2011;141:1194–1201.
13. Serada S, Fujimoto M, Ogata A, et al. iTRAQ-based proteomic identification of leucine-rich alpha-2 glycoprotein as a novel inflammatory biomarker in autoimmune diseases. *Ann Rheum Dis*. 2010;69:770–774.
14. Haupt H, Baudner S. Isolation and characterization of an unknown, leucine-rich 3.1-S-alpha2-glycoprotein from human serum [author's transl]. *Hoppe Seylers Z Physiol Chem*. 1977;358:639–646.
15. Takahashi N, Takahashi Y, Putnam FW. Periodicity of leucine and tandem repetition of a 24-amino acid segment in the primary structure of leucine-rich alpha 2-glycoprotein of human serum. *Proc Natl Acad Sci U S A*. 1985;82:1906–1910.
16. Shirai R, Hirano F, Ohkura N, et al. Up-regulation of the expression of leucine-rich alpha(2)-glycoprotein in hepatocytes by the mediators of acute-phase response. *Biochem Biophys Res Commun*. 2009;382: 776–769.
17. O'Donnell LC, Druhan LJ, Avalos BR. Molecular characterization and expression analysis of leucine-rich alpha2-glycoprotein, a novel marker of granulocytic differentiation. *J Leukoc Biol*. 2002;72: 478–485.
18. Rachmilewitz D. Coated mesalazine (5-aminosalicylic acid) versus sulphasalazine in the treatment of active ulcerative colitis: a randomised trial. *BMJ*. 1989;298:82–86.
19. Kruis W, Schreiber S, Theuer D, et al. Low dose balsalazide (1.5 g twice daily) and mesalazine (0.5 g three times daily) maintained remission of ulcerative colitis but high dose balsalazide (3.0 g twice daily) was superior in preventing relapses. *Gut*. 2001;49:783–789.
20. Matts SG. The value of rectal biopsy in the diagnosis of ulcerative colitis. *Q J Med*. 1961;30:393–407.
21. Iwahori K, Serada S, Fujimoto M, et al. Overexpression of SOCS3 exhibits preclinical antitumor activity against malignant pleural mesothelioma. *Int J Cancer*. 2011;129:1005–1017.
22. Kim A, Enomoto T, Serada S, et al. Enhanced expression of Annexin A4 in clear cell carcinoma of the ovary and its association with chemoresistance to carboplatin. *Int J Cancer*. 2009;125:2316–2322.
23. Fujimoto M, Nakano M, Terabe F, et al. The influence of excessive IL-6 production in vivo on the development and function of Foxp3+ regulatory T cells. *J Immunol*. 2011;186:32–40.
24. Murch SH, Lamkin VA, Savage MO, et al. Serum concentrations of tumour necrosis factor alpha in childhood chronic inflammatory bowel disease. *Gut*. 1991;32:913–917.
25. Woywodt A, Ludwig D, Neustock P, et al. Mucosal cytokine expression, cellular markers and adhesion molecules in inflammatory bowel disease. *Eur J Gastroenterol Hepatol*. 1999;11:267–276.
26. Andoh A, Zhang Z, Inatomi O, et al. Interleukin-22, a member of the IL-10 subfamily, induces inflammatory responses in colonic subepithelial myofibroblasts. *Gastroenterology*. 2005;129:969–984.
27. Okayasu I, Hatakeyama S, Yamada M, et al. A novel method in the induction of reliable experimental acute and chronic ulcerative colitis in mice. *Gastroenterology*. 1990;98:694–702.
28. Kentsis A, Lin YY, Kurek K, et al. Discovery and validation of urine markers of acute pediatric appendicitis using high-accuracy mass spectrometry. *Ann Emerg Med*. 2010;55:62–70 e4.

E X D	1 4 5 4	B	Dispatch: 3.2.12	Journal: EXD	CE: Deepika K
Journal Name	Manuscript No.		Author Received:	No. of pages: 6	PE: Sathya Kala

DOI:10.1111/j.1600-0625.2012.01454.x
www.blackwellpublishing.com/EXD

Original Article

Periostin, a matricellular protein, accelerates cutaneous wound repair by activating dermal fibroblasts

Kanako Ontsuka[1*], Yorihisa Kotobuki[2,3*], Hiroshi Shiraishi[1], Satoshi Serada[3], Shoichiro Ohta[4], Atsushi Tanemura[2], Lingli Yang[2,3], Minoru Fujimoto[3], Kazuhiko Arima[1], Shoichi Suzuki[1], Hiroyuki Murota[2], Shuji Toda[5], Akira Kudo[6], Simon J. Conway[7], Yutaka Narisawa[8], Ichiro Katayama[2], Kenji Izuhara[1] and Tetsuji Naka[3]

[1]Division of Medical Biochemistry, Department of Biomolecular Sciences, Saga Medical School, Saga, Japan; [2]Department of Dermatology, Osaka University Graduate School of Medicine, Suita, Japan; [3]Laboratory for Immune Signal, National Institute of Biochemical Innovation, Ibaraki, Japan; [4]Department of Laboratory Medicine, Saga Medical School, Saga, Japan; [5]Department of Pathology and Biodefense, Saga Medical School, Saga, Japan; [6]Department of Biological Information, Tokyo Institute of Technology, Yokohama, Japan; [7]Program in Developmental Biology and Neonatal Medicine, Herman B. Wells Center for Pediatric Research, Indiana University School of Medicine, Indianapolis, IN, USA; [8]Department of Dermatology, Saga Medical School, Saga, Japan

Correspondence: Kenji Izuhara, Division of Medical Biochemistry, Department of Biomolecular Sciences, Saga Medical School, 5-1-1, Nabeshima, Saga 849-8501, Japan, Tel.: +81-952-34-2261, Fax: +81-952-34-2058, e-mail: kizuhara@cc.saga-u.ac.jp

**These two authors contributed equally to this work.*

Abstract: Cutaneous wound repair is a highly ordered and well-coordinated process involving various cell lineages and many molecular effectors. Cell–matrix interactions through integrin molecules provide key signals important for wound repair. Periostin is a matricellular protein that may provide signals important during tissue development and remodelling by interacting with several integrin molecules, via the phosphatidylinositol 3-kinase/Akt and MAP kinase pathways. In this study, we examined the role of periostin in the process of cutaneous wound repair using periostin-deficient mice and by analysing the effects of periostin on dermal fibroblasts. We first determined the expression profile and localization of periostin in a well-characterized wound repair model mice. Periostin was robustly deposited in the granulation tissues beneath the extended epidermal wound edges and at the dermal–epidermal junctions in wounded mice. Moreover, periostin-deficient mice exhibited delayed *in vivo* wound repair, which could be improved by direct administration of exogenous periostin. *In vitro* analyses revealed that loss of periostin impaired proliferation and migration of dermal fibroblasts, but exogenous supplementation or enforced periostin expression enhanced their proliferation. Combined, these results demonstrate that periostin accelerates the process of cutaneous wound repair by activating fibroblasts.

Key words: fibroblast – matrix – mice – periostinintegrin – wound repair

Accepted for publication 18 January 2012

Introduction

Cutaneous wound repair is a physiological function that is well ordered and highly coordinated (1–4). The process of repair is divided into three phases: inflammation, new tissue formation and remodelling. In the inflammatory phase beginning with haemostasis, first neutrophils and later macrophages are recruited to the wound site. These infiltrated macrophages not only exert their phagocytic activities but also accelerate re-epithelialization and granulation tissue formation. During new tissue formation, the process of re-epithelialization occurs via extension of wedge-shaped keratinocyte lineage. Fibroblasts and macrophages subsequently form the granulation tissues, assisting in the key process of re-epithelialization. Finally, during the remodelling phase, most of the endothelial cells, macrophages and myofibroblasts undergo apoptosis, leaving a scar containing a few cells with an extensive extracellular matrix (ECM) deposition dominated by collagens.

In the new tissue forming phase, fibroblasts produce mainly collagens and other ECM components such as glycosaminoglycans and proteoglycans, contributing to the formation of granulation tissues, with the provisional fibrin-based matrix eventually being replaced (1,5–7). In addition, fibroblasts secrete various growth factors – fibroblast growth factor-2 (FGF-2)/basic FGF, FGF-7/keratinocyte growth factor, FGF-10, epidermal growth factor and transforming growth factor-β (TGF-β) – which can all affect the process of keratinocyte re-epithelialization (8). TGF-β1 can also drive differentiation of some fibroblasts into transformed myofibroblasts that express α-smooth muscle actin (α-SMA) (9), which are able to contract to draw the wound edges together (1–4). This combination of growth factor receptor–mediated signals and integrin-mediated signals are thought to result in growth, migration, survival, spreading and ECM production responses within the wound fibroblasts (10–12). However, the underlying mechanism of fibroblast activation during cutaneous wound repair has not yet been fully understood.

Periostin is an ECM protein belonging to the fasciclin family (13,14) and is a newly characterized matricellular protein whose main functions are thought to be modulation of cell–matrix interactions and cell functions rather than playing a direct structural role (15,16). Periostin is known to interact with several integrin molecules, specifically $\alpha_v\beta_3$ or $\alpha_v\beta_5$ on cell surfaces, activating the phosphatidylinositol 3-kinase (PI3K)/Akt and MAP kinase pathways during tissue development and remodelling (13,14). We and others have demonstrated the presence of periostin in fibrotic areas in various pathological conditions: bronchial

asthma (17–19), pulmonary fibrosis (20), myocardial infarction (21), valvular heart disease (22), cystic fibrosis (23) and proliferative diabetic retinopathy (24). Further, it has been shown that the biological functions of periostin as a matricellular protein rather than structural player are important for the pathogenesis of some of these diseases. For instance, periostin affects eosinophils and/or epithelial cells in bronchial asthma, enhancing eosinophil migration and/or activating TGF-β, respectively (25,26). Moreover, in the healing process of myocardial infarction, periostin may enhance cardiac repair via stimulation of myocyte proliferation (27), although whether this is a direct mechanism or via adjacent cardiac fibroblasts remains controversial (28). Furthermore, periostin accelerates the development of various tumors by promoting cancer cell survival, epithelial–mesenchymal transition, invasion and metastasis (29,30). In contrast, the physiological roles of periostin remain poorly understood, except for several studies using periostin-deficient mice that suggest non-replaceable roles for periostin during development of bone, tooth and heart valves (14,31).

Importantly for this study, periostin is known to be highly expressed in wounds, suggesting its involvement in the process of wound repair (32,33). To directly examine the role of periostin within the process of cutaneous wound repair, we employed both *in vivo* and *in vitro* approaches using systemic periostin-deficient mice, exogenous periostin supplementation and a well-characterized mouse wound repair model. Significantly, wound repair is delayed in periostin-deficient mice. Furthermore, exogenous periostin up-regulates proliferation and migration of the dermal fibroblasts, which suggests this may be the mechanism how periostin accelerates cutaneous wound repair. These results demonstrate that periostin is required for the process of cutaneous wound repair, highlighting its physiological role, and suggest that periostin may be a useful candidate to therapeutically speedup wound repair.

Methods

Mice

Eight- to twelve-week-old C57BL/6 or BALB/c mice (Japan SLC, Japan), periostin-deficient (*Postn*$^{-/-}$, C57BL/6 or BALB/c background) mice, were used (14,21). Experiments were undertaken following the guidelines for care and use of experimental animals required by the Japanese Association for Laboratory Animals Science (1987).

Mouse wound repair model

Mice were anaesthetized by inhalation of halothane or intraperitoneal injection of pentobarbital. After their backs were shaved, 8- or 10-mm diameter full-thickness wounds were generated using disposable biopsy punches (Kai Industries, Seki, Japan). Wound sizes were measured longitudinally with a slide calliper. Wound tissues were excised at indicated time points postinjury and used for quantitative RT-PCR, Western blotting or histological analysis. Following fixation in 3.7% formaldehyde and embedding in paraffin, histological analysis was performed on serial sections from spanning the central portion of the wound and stained with haematoxylin and eosin (H&E), Masson's trichrome and/or via immunohistochemical staining as previously described (18,20). In selected experiments, 2 μg recombinant mouse periostin (R&D Systems, Minneapolis, MN, USA) was painted onto the wound lesions every 2 days from day 1 to 9.

Quantitative RT-PCR

Quantitative RT-PCR was used to measure periostin as previously described (18). Briefly, RNA from wound site was isolated using an RNeasy Mini kit (Qiagen Japan, Tokyo, Japan), and the RT reaction was performed using a QuantiTect Reverse Transcription Kit (Qiagen Japan). Quantitative analysis was achieved using Applied Biosystems StepOnePlus™ Real-Time PCR System (Life Technologies Japan, Tokyo, Japan). The primer sequence and PCR conditions are referred to the Data S1.

Confocal microscopy

Excised wound tissues were fixed with 3.7% formaldehyde and embedded in paraffin. After blocking with 2% BSA, the wax sections were stained using polyclonal anti-periostin Ab, previously prepared (18) followed by Alexa488-labelled anti-rabbit IgG Ab (Invitrogen, Carlsbad, CA, USA). The sections were mounted by Dako fluorescent mounting medium (Dako, Glostrup, Denmark) and then examined by LSM5 PASCAL G/B microscope (Carl Zeiss Japan, Tokyo, Japan).

Transduction of periostin into MEFs

Mouse full-length *Postn* cDNA was cloned (ENSMUST000000-81564) from MEF. Overexpression of mouse periostin into wild-type or periostin-deficient MEFs was performed using retroviral transduction of pMXs-puro vector [provided by Dr. Toshio Kitamura, Tokyo University, Tokyo, Japan (34)]. As a control, an empty vector was used alongside periostin-containing vector. After transduction, only infected cells were selected by 1 μg/ml puromycin (InvivoGen, San Diego, CA, USA).

Proliferation assay

Proliferation of fibroblasts was examined using the Cell Counting Reagent SF (Nacalai Tesque, Kyoto, Japan) according to the manufacturer's recommendations. In selected experiments, after 4-h serum starvation, dermal fibroblasts were seeded on the specified concentration of recombinant periostin (as described previously).

Statistical analyses

The results are presented as means + SD. Analysis was carried out using the two-sided, unpaired Student's *t*-test or the two-sided Welch test. Multiple comparisons between groups were performed by Fisher's or Dunnett's methods. We considered values to be significant when $P < 0.05$.

Results

Periostin expression is induced in wound tissues

We first analysed the expression of periostin in wound tissues. In C57BL/6 mice, periostin mRNA started to increase at day 1 after injury and peaked at day 7, decreasing thereafter (Fig. 1a, $n = 8$). Correspondingly, periostin protein levels peaked at day 7–10 and were sustained until day 18 (Fig. 1b). Wounded mice on the BALB/c background showed almost identical kinetics of periostin temporal changes at both the mRNA and protein levels (Fig. S1, $n = 8$). We then examined whether the localization of periostin was altered in wounded tissues. In the normal unwounded skin, periostin was expressed weakly at the dermal–epidermal junction and relatively robustly around the hair follicles (Figs 1c and S2). At day 6, when the wound was still open with hypertrophic epidermal wound edges and granulation tissues formed beneath these edges, periostin was now strongly expressed in the dermal–epidermal junction at these edges and within the granulation tissues. At day 9, when the wound was closed, significant expression of periostin was still observed in the granulation tissues beneath

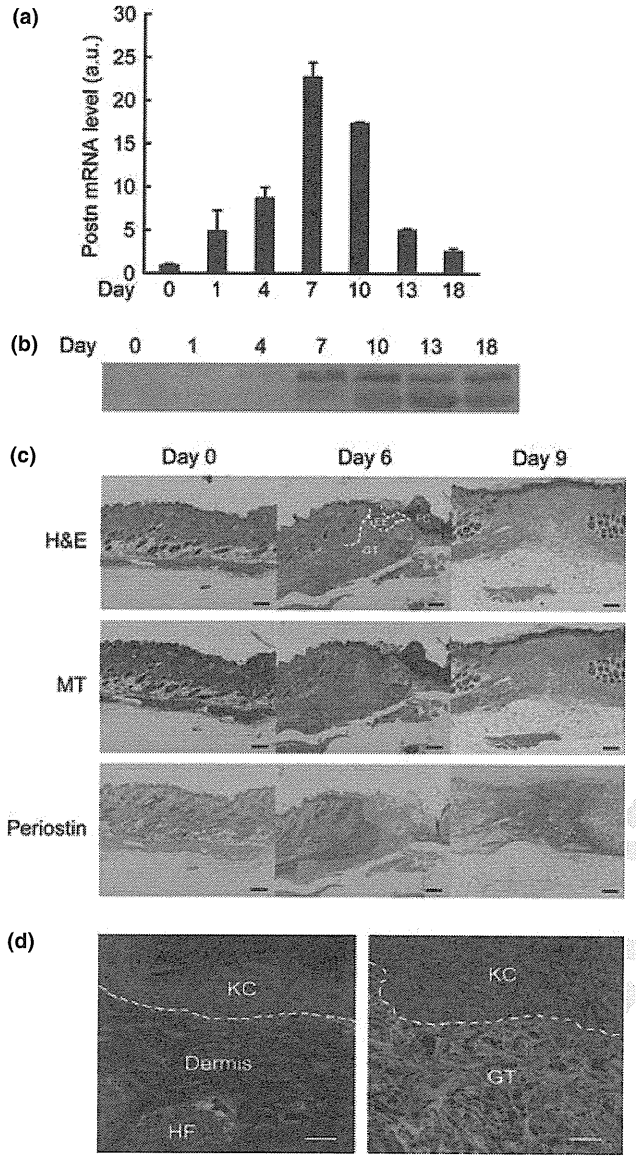

Figure 1. Periostin expression in wounded tissues. (a, b) Analysis of expression of periostin mRNA (a) or periostin protein (b) in wounded skin of C57BL/6 (n = 8) mice following the indicated amount of days postinjury. In b, experiments were repeated three times, and the representative combined data are depicted. (c) Wound sites stained with H&E, Masson trichrome (MT) and anti-periostin Ab from wild-type C57BL/6 mice for the indicated amount of days postinjury. FC, fibrin clot; EE, epidermal edge; GT, granulation tissue. Scale bar represents 200 μm. (d) Confocal microscopic imaging of wounds at day 6 is shown. Left and right panels depict non-wounded or wounded areas, respectively. Green and red represent periostin and the intrinsic fluorescence of cells, respectively. Scale bar represents 20 μm. KC, keratinocyte; GT, granulation tissue; HC, hair follicle.

the re-epithelialized wounds. To assess localization, we double-stained periostin (appears green), and this enabled us to conclude that periostin was deposited only at the border between the epidermis and the dermis and around hair follicles in the non-wounded sites, whereas periostin was deposited in the interspace regions of the red-staining granulation tissues in the wounded sites (Fig. 1d). These results demonstrate that periostin is induced during wound repair, suggesting that periostin may play a role in the repair process as well as being a useful marker of well-organized wound repair.

Periostin is required for efficient wound repair in mice

To test the functional requirement of periostin in wound repair, we used periostin-deficient ($Postn^{-/-}$) mice to perform wounding and assess their response. The wound sizes during the healing time course were significantly reduced in $Postn^{+/+}$ mice in C57BL/6 background (Fig. 2a,b, n = 10 for each genotype, $P < 0.05$ at day 3, 5 and 11, $P < 0.01$ at day 7) and in $Postn^{+/-}$ mice in a BALB/c background (Fig. S3, n = 3 for $Postn^{-/-}$ and n = 6 for $Postn^{+/-}$, $P < 0.05$ at day 3 and 10, $P < 0.001$ at day 13) than those observed in age-matched litter $Postn^{-/-}$ mice. Accordingly, the time intervals to completely close the wounds were significantly extended in $Postn^{-/-}$ mice than within $Postn^{+/+}$ mice (Fig. S4, 14.1 ± 0.74 days vs 15.9 ± 1.6 days, $P < 0.05$).

When we painted recombinant periostin protein onto the wounded area of $Postn^{-/-}$ mice every 2 days, starting day 1 after injury to day 9, the observed slower wound repair was subsequently accelerated (Fig. 2c,d upper panel, n = 10 for each group, the wound sizes: $P < 0.01$ at day 3, $P < 0.001$ at day 5 and 7, the time interval required to close the wounds: 15.9 ± 1.6 days vs 13.8 ± 1.4 days, $P < 0.01$). Moreover, the effects of administering exogenous periostin on accelerating wound repair were observed even in $Postn^{+/+}$ mice (Fig. 2c lower panel and Fig. S4, the wound sizes: $P < 0.05$ at day 7, the time interval to close the wounds: 14.1 ± 0.74 days vs 12.8 ± 1.1 days, $P < 0.01$). Thus, these results clearly demonstrate the requirement and positive effect of periostin within the wound repair process in mice.

Effect of periostin on proliferation in dermal fibroblasts

It has been shown that periostin can bind $\alpha_v\beta_3$ and $\alpha_v\beta_5$ integrin heterodimers (13,14) and that signalling via integrin molecules is imperative for cell proliferation and migration (10–12). Thus, we confirmed that α_v, β_3 and β_5 integrins, but not β_4 integrin, were expressed in human dermal fibroblasts, although A431 cells express β_4 integrin (Fig. S5A). Furthermore, when we stimulated human dermal fibroblasts with recombinant periostin, phosphorylation of downstream molecules of integrins focal adhesion kinase [FAK, STAT3, Akt and p44/42MAPK] was also observed (Fig. S5B). These results suggest that the interaction of periostin with human dermal fibroblasts is able to activate key signalling pathways via integrins present in the wound.

The present observation that periostin was strongly deposited within the granulation tissues beneath the hypertrophic epidermal wound edges raised the possibility that periostin may directly affect fibroblast proliferation, thereby accelerating the repair process. To explore this possibility, we initially examined the effects of exogenous periostin on proliferation of normal human dermal fibroblasts (NHDFs). We confirmed that NHDFs proliferate in response to FGF2 (Fig. S6). We also found that proliferation of NHDFs was up-regulated in a dose-dependent manner of periostin coated on plates (Fig. 3a, $P < 0.05$ at periostin 0.1 μg/ml, 24 h, $P < 0.01$ at periostin 1 μg/ml, 24 h, $P < 0.001$ at periostin 0.1 or 1 μg/ml, 72 h and at periostin 0.1 or 1 μg/ml, 120 h). We then analysed the effects of periostin deficiency on proliferative activities of mouse dermal fibroblasts. Fibroblast cultures established from skin of newborn $Postn^{-/-}$ mice had impaired proliferation compared with fibroblasts from $Postn^{+/+}$ mice (Fig. 3b, $P < 0.05$ at 6 and 48 h, $P < 0.01$ at 24 h, $P < 0.001$ at 72 h). Treatment

with recombinant periostin slightly enhanced proliferation of fibroblasts from both wild-type (Fig. 3c, $P < 0.05$ at 72 h) and periostin-deficient ($P < 0.05$ at 12 and 24 h) mice. Further, we overexpressed retrovirally periostin in periostin-deficient fibroblasts and in wild-type fibroblasts (Fig. S7). As expected, these periostin-overexpressed cells had significantly up-regulated proliferation compared with mock-transfected wild-type (Fig. 3d, $P < 0.001$ at 24, 48, 60 and 72 h) or periostin-deficient (Fig. 3d, $P < 0.01$ at 60 and 72 h, $P < 0.001$ at 24 and 48 h) fibroblasts, respectively. These *in vitro* data demonstrate that either exogenously added or ectopically expressed periostin enhances the proliferative activities of fibroblasts.

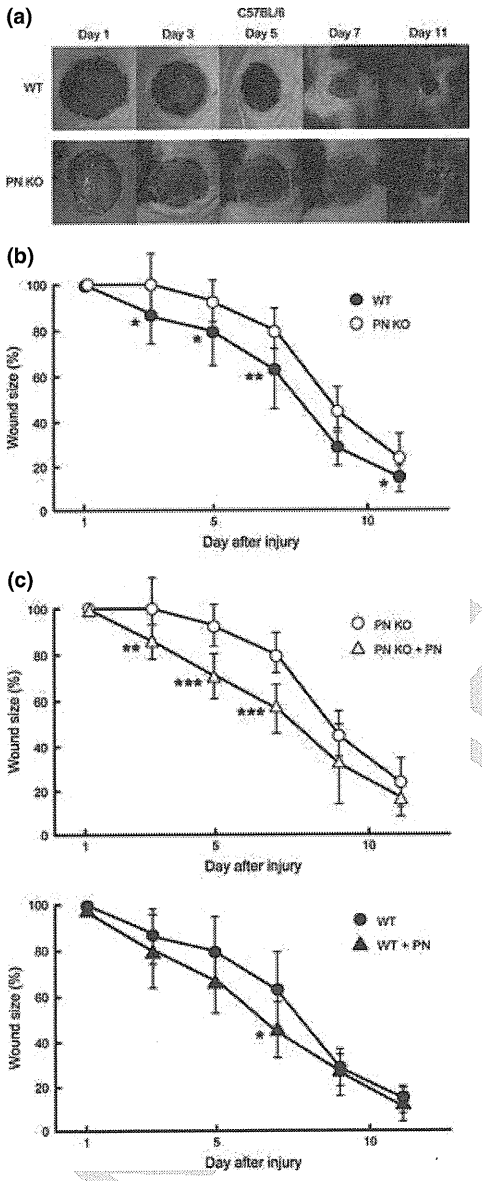

Figure 2. Periostin is important for efficient wound healing in mice. Successive photographs of the wounds (a), wound sizes at the indicated amount of days postinjury (b) in wild-type (WT, $n = 10$), or periostin-deficient mice (PN KO, $n = 10$) in C57BL/6 background. (c) Recombinant human periostin (+PN 2 μg) was injected intradermally into wounds of C57BL/6 background mice ($n = 10$ for each of WT and PN KO) every 2 days, from day 1 after injury to day 9. Wound sizes at the indicated times after injury (c). Statistical differences between PN KO vs WT, PN KO + PN vs PN KO and WT + PN vs WT are depicted. $^{*}P < 0.05$, $^{**}P < 0.01$, $^{***}P < 0.001$.

Periostin enhances migration of dermal fibroblasts

We then examined the effects of periostin on migration of dermal fibroblasts using scratch wound cell monolayer method in wild-type and periostin-deficient MEFs (Fig. 4a,b). To exclude confounding effects upon proliferation, we arrested cell growth prior to analysis of migration. We confirmed that the migration activity of wild-type MEFs was up-regulated by platelet-derived growth factor (PDGF), whereas that was down-regulated by cytochalasin D (Fig. S8). The motility of periostin-deficient MEFs was significantly impaired compared with that of wild-type MEFs ($P < 0.05$ at 24 h). These results demonstrate that periostin can also enhance migration as well as the proliferation status of fibroblasts in response to wounding.

Discussion

It is well recognized that the ECM regulates the functions of the various cell lineages mobilized to the wounded area, contributing not only to re-epithelialization but also to granulation tissue formation and angiogenesis (35). Moreover, several studies using genetically deficient mice have shown that ECM proteins can play important *in vivo* functions during wounding and repair. For instance, fibronectin and its co-receptor, syndecan-4, are thought to accelerate wound repair as loss-of-function mouse mutants defective in the extra domain A of fibronectin or syndecan-4 both exhibit delayed cutaneous wound repair (36,37), whereas thrombospondin-1 and -2 play an opposite role and mainly inhibit wound repair (38,39). Based on previous observations that periostin is an ECM protein highly expressed during wound repair in various mouse models (32,33), in this study, we used periostin-deficient mice to test its requirement via our wound repair model. Meaningfully, both *in vivo* and *in vitro* results support the conclusion that periostin accelerates the wound healing process. Recently, using periostin-deficient mice, Nishiyama et al. (40) also reported that lack of periostin delays the process of cutaneous wound repair. Taking these results together, the requirement of periostin for the process of efficient cutaneous wound repair is well established.

The Nishiyama et al. (40) data indicated that periostin up-regulates keratinocyte proliferation and migration, accelerating the process of re-epithelialization. This result is consistent with our observation of significant periostin expression observed in the dermal–epidermal junction during wound repair. In our study, we similarly demonstrate that periostin enhances proliferation and migration of fibroblasts, which would contribute to the process of granulation tissue formation. We also demonstrated that periostin is deposited in fibroblast-enriched granulation tissues. Fibroblasts contribute to wound repair by generating several growth factors important for re-epithelialization (8) and by differentiating into α-SMA-expressing myofibroblasts important to close the wound edges by TGF-β1 (1–4). Collectively, these suggest that periostin deposition and the formation of fibroblast-enriched granulation tissues is the critical step during wound repair. The significance of fibroblast activation during wound repair is also supported by data from profibrotic cytokine, FGF2-null mice (41). Therefore, it is likely that direct or indirect activation of dermal fibroblasts by presence of periostin may be an additional mechanism underlying

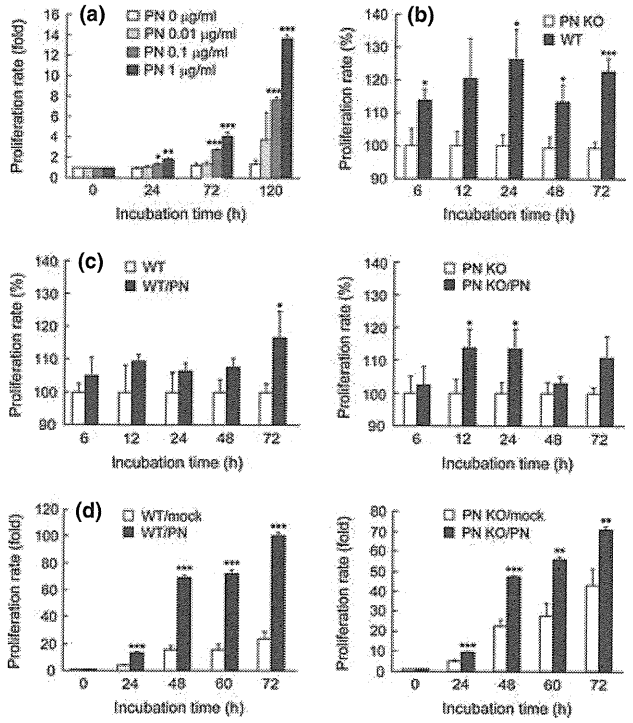

Figure 3. Effects of periostin on fibroblast proliferation. (a–c) Normal human dermal fibroblasts (a) or mouse dermal fibroblasts derived from wild-type (WT) or periostin-deficient mice (PN KO) (b, c) were cultured for various times. In panel (a), the concentrations of human periostin used are indicated, and in panel (c), 100 ng/ml of mouse periostin was used to coat the culture dishes. (d) Mouse periostin-overexpressed or mock-transduced MEFs (3×10^3 cells) derived from wild-type (WT) or periostin-deficient (PN KO) mice were cultured for various lengths. The proliferation rate was estimated using the Cell Counting Reagent SF. The relative folds were compared with the starting points (a, d) or PN KO-type or to fibroblasts on non-coated plates (b, c) are depicted. In panel (a), one-way ANOVA followed by Dunnett's test was used for multiple comparisons of the different fibroblast rates induced by various concentrations of periostin. Statistical differences were compared with PN 0 ng/ml cultures. Experiments were repeated five times, and the representative combined data are depicted. $*P < 0.05$, $**P < 0.01$, $***P < 0.001$.

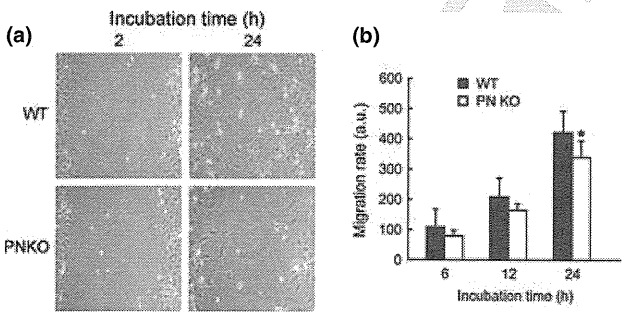

Figure 4. Effects of periostin on the migration of fibroblasts. Analysis of cell migration in MEFs derived from wild-type (WT) or periostin-deficient (PN KO) mice were compared. Photographs of the wounded cell monolayers at 2 and 24 h (a) and the relative cell motilities at various times indicated (b). The average cell motility (14 points per one field and three different fields/well in triplicate) was calculated and shown. Statistical difference between WT vs PN KO ($*P < 0.05$) is depicted.

wound repair, in addition to periostin activation of keratinocytes (40).

It is well known that TGF-β1 is highly expressed in wounded tissues and can act as a central enhancer of wound repair effectors (42,43). Consequently, mice deficient in TGF-β1 show delayed cutaneous wound repair (44). When we examined whether TGF-β1 or other cytokines were able to directly induce periostin expression in human dermal fibroblasts and accumulated periostin in the supernatant was seen in responses to IL-4 and IL-13 (17,18) and to TGF-β1, whereas several other cytokines (IL-1β, -6, -17, tumor necrosis factor-α, FGF-2, FGF-5, stromal cell-derived factor-1, and PDGF) were not able to induce periostin expression (Fig. S9). Collectively, these results suggest that TGF-β1, abundant in the wound site, mainly contributes to periostin induction and that induction of periostin is a novel biological function of TGF-β1 within the well-ordered process of wound repair.

Targeted genetic deletion of periostin in mice significantly impairs fibroblast proliferation and wound healing, whereas fibroblast proliferation and wound healing can be enhanced by exogenous periostin, suggesting a direct role for periostin. Furthermore, treatment of dermal fibroblasts with exogenous periostin activates integrin-associated signalling molecules (FAK, STAT3, Akt and p44/42MAPK). As integrin-mediated signalling is initiated by formation of the Src/FAK complex, which enhances cell proliferation by up-regulating cyclin D1 expression via p44/42MAPK or cell survival by inhibiting proapoptotic factors such as Bad, caspase nine, forkhead transcription factors via PI3K/Akt (10–12), our results indicate that several levels of the proliferation pathway are activated when periostin is present. Moreover, STAT3 transduces signals important for cell proliferation and survival, cooperating with growth factor receptor-mediated signals (45,46). Periostin has been shown to induce proliferation of smooth muscle and/or cancer cells via the FAK/PI3K/Akt pathway (47,48). In contrast, genetic inhibition or administration of MAPK inhibitors delays wound repair (49,50). Finally, direct activation of the PI3K/Akt pathway is known to accelerate wound repair (51). These collective results suggest that periostin–integrins signal via FAK, STAT3, Akt and p44/42MAPK and play an important role in wound repair via augmenting cell proliferation/survival.

Clinically, it may be imperative to modulate either delayed (e.g. from diabetes or radiation exposure) or enhanced wound repair [e.g. hypertrophic and keloid scars (2,3)]. However, disappointing clinical results from single-agent therapies such as administering growth factors or other mediators to boost wound repair suggest that it is a highly ordered and complex process. Our surprising result, that injection of periostin into the wound in mice models can accelerate the healing process, may suggest that topical administration of periostin could be efficacious in wound treatment. Furthermore, it is now hoped that recent advances in stem cell/progenitor cell biology and material sciences will make it possible to entirely replace tissues. Our present data regarding the role of periostin in wound repair indicate that it could be a useful addition in construction of optimized skin tissues.

In conclusion, in this study, we demonstrate that periostin, transiently expressed during wound repair, accelerates the process by activating dermal fibroblasts. Although the pathological roles of periostin within fibrosis in various diseases have recently been well characterized, the physiological roles of periostin in skin repair are starting to be uncovered. Our present study demonstrates a novel physiological role for periostin: namely, its involvement in effective cutaneous wound repair.

Acknowledgements

We thank Dr. Dovie R. Wylie, Hiroyuki Ideguchi, Yumiko Ohishi, Yukako Kanazawa and Maiko Urase for critical review of this manuscript, technical and secretarial assistance. KO, YK, HS, SS and LY performed the research. AT, MF, YN, HM, ST, IK, KI and TN designed the research study. SO, KA, SS, AK and SJC contributed essential reagents or tools. KO, YK, SJC and KI wrote the paper. This work was supported in part by Grants-in-Aid for Scientific Research from the Japan Society for the Promotion of Science and by Grant-in-Aid from the Ministry of Health, Labour and Welfare, Japan.

Conflict of interests

The authors have no declared no conflicts of interests.

References

1 Baum C L, Arpey C J. Dermatol Surg 2005: **31**: 674–686.
2 Gurtner G C, Werner S, Barrandon Y *et al.* Nature 2008: **453**: 314–321.
3 Singer A J, Clark R A. N Engl J Med 1999: **341**: 738–746.
4 Palatinus J A, Rhett J M, Gourdie R G. J Mol Cell Cardiol 2010: **48**: 550–557.
5 Ranzato E, Martinotti S, Volante A *et al.* Exp Dermatol 2011: **20**: 308–313.
6 Kim J H, Jung M, Kim H S *et al.* Exp Dermatol 2011: **20**: 383–387.
7 Novotny M, Vasilenko T, Varinska L *et al.* Exp Dermatol 2011: **20**: 703–708.
8 Werner S, Grose R. Physiol Rev 2003: **83**: 835–870.
9 Desmouliere A, Geinoz A, Gabbiani F *et al.* J Cell Biol 1993: **122**: 103–111.
10 Eliceiri B P. Circ Res 2001: **89**: 1104–1110.
11 Giancotti F G, Ruoslahti E. Science 1999: **285**: 1028–1032.
12 Hynes R O. Trends Cell Biol 1999: **9**: M33–M37.
13 Hamilton D W. J Cell Commun Signal 2008: **2**: 9–17.
14 Rios H, Koushik S V, Wang H *et al.* Mol Cell Biol 2005: **25**: 11131–11144.
15 Midwood K, Sacre S, Piccinini A M *et al.* Nat Med 2009: **15**: 774–780.
16 Shinohara M L, Kim J H, Garcia V A *et al.* Immunity 2008: **29**: 68–78.
17 Hayashi N, Yoshimoto T, Izuhara K *et al.* Proc Natl Acad Sci U S A 2007: **104**: 14765–14770.
18 Takayama G, Arima K, Kanaji T *et al.* J Allergy Clin Immunol 2006: **118**: 98–104.
19 Woodruff P G, Boushey H A, Dolganov G M *et al.* Proc Natl Acad Sci U S A 2007: **104**: 15858–15863.
20 Okamoto M, Hoshino T, Kitasato Y *et al.* Eur Respir J 2011: **37**: 1119–1127.
21 Shimazaki M, Nakamura K, Kii I *et al.* J Exp Med 2008: **205**: 295–303.
22 Hakuno D, Kimura N, Yoshioka M *et al.* J Clin Invest 2010: **120**: 2292–2306.
23 Oku E, Kanaji T, Takata Y *et al.* Int J Hematol 2008: **88**: 57–63.
24 Yoshida S, Ishikawa K, Asato R *et al.* Invest Ophthalmol Vis Sci 2011: **52**: 5670–5678.
25 Blanchard C, Mingler M K, McBride M *et al.* Mucosal Immunol 2008: **1**: 289–296.
26 Sidhu S S, Yuan S, Innes A L *et al.* Proc Natl Acad Sci U S A 2010: **107**: 14170–14175.
27 Kuhn B, del Monte F, Hajjar R J *et al.* Nat Med 2007: **13**: 962–969.
28 Lorts A, Schwanekamp J A, Elrod J W *et al.* Circ Res 2009: **104**: e1–e7.
29 Fujimoto K, Kawaguchi T, Nakashima O *et al.* Oncol Rep 2011: **25**: 1211–1216.
30 Ruan K, Bao S, Ouyang G. Cell Mol Life Sci 2009: **66**: 2219–2230.
31 Snider P, Hinton R B, Moreno-Rodriguez R A *et al.* Circ Res 2008: **102**: 752–760.
32 Jackson-Boeters L, Wen W, Hamilton D W. J Cell Commun Signal 2009: **3**: 125–133.
33 Zhou H M, Wang J, Elliott C *et al.* J Cell Commun Signal 2010: **4**: 99–107.
34 Kitamura T, Koshino Y, Shibata F *et al.* Exp Hematol 2003: **31**: 1007–1014.
35 Midwood K S, Williams L V, Schwarzbauer J E. Int J Biochem Cell Biol 2004: **36**: 1031–1037.
36 Echtermeyer F, Streit M, Wilcox-Adelman S *et al.* J Clin Invest 2001: **107**: R9–R14.
37 Muro A F, Chauhan A K, Gajovic S *et al.* J Cell Biol 2003: **162**: 149–160.
38 Kyriakides T R, Tam J W, Bornstein P. J Invest Dermatol 1999: **113**: 782–787.
39 Streit M, Velasco P, Riccardi L *et al.* EMBO J 2000: **19**: 3272–3282.
40 Nishiyama T, Kii I, Kashima T G *et al.* PLoS One 2011: **6**: e18410.
41 Ortega S, Ittmann M, Tsang S H *et al.* Proc Natl Acad Sci U S A 1998: **95**: 5672–5677.
42 Barrientos S, Stojadinovic O, Golinko M S *et al.* Wound Repair Regen 2008: **16**: 585–601.
43 Werner S, Krieg T, Smola H. J Invest Dermatol 2007: **127**: 998–1008.
44 Crowe M J, Doetschman T, Greenhalgh D G. J Invest Dermatol 2000: **115**: 3–11.
45 Guo W, Pylayeva Y, Pepe A *et al.* Cell 2006: **126**: 489–502.
46 Shin H D, Park B L, Kim L H *et al.* Hum Mol Genet 2004: **13**: 397–403.
47 Bao S, Ouyang G, Bai X *et al.* Cancer Cell 2004: **5**: 329–339.
48 Li G, Jin R, Norris R A *et al.* Atherosclerosis 2010: **208**: 358–365.
49 Sharma G D, He J, Bazan H E. J Biol Chem 2003: **278**: 21989–21997.
50 Thuraisingam T, Xu Y Z, Eadie K *et al.* J Invest Dermatol 2010: **130**: 278–286.
51 Lai J P, Dalton J T, Knoell D L. Br J Pharmacol 2007: **152**: 1172–1184.

Supporting Information

Additional Supporting Information may be found in the online version of this article:

Figure S1. Periostin expression in wounded tissues.

Figure S2. Expression of periostin in the wound sites in mice.

Figure S3. Periostin is important for efficient wound healing in mice.

Figure S4. Periostin is important for efficient wound healing in mice.

Figure S5. Activation of human dermal fibroblasts by exogenous periostin.

Figure S6. Effects of fibroblast growth factor-2 on fibroblast proliferation.

Figure S7. Establishment of periostin-transduced MEFs.

Figure S8. Effects of cytochalasin D and platelet-derived growth factor on cell migration.

Figure S9. Analysis of periostin responses in human dermal fibroblasts to various stimuli.

Data S1. Materials and methods.

Please note: Wiley-Blackwell is not responsible for the content or functionality of any supporting materials supplied by the authors. Any queries (other than missing material) should be directed to the corresponding author for the article.

Pigment Cell Melanoma Res. **25**; 219–230

ORIGINAL ARTICLE

Dysregulation of melanocyte function by Th17-related cytokines: significance of Th17 cell infiltration in autoimmune vitiligo vulgaris

Yorihisa Kotobuki[1,2,*], Atsushi Tanemura[1,*], Lingli Yang[1,2], Saori Itoi[1], Mari Wataya-Kaneda[1], Hiroyuki Murota[1], Minoru Fujimoto[2], Satoshi Serada[2], Tetsuji Naka[2] and Ichiro Katayama[1]

1 Department of Dermatology Integrated Medicine, Osaka University Graduate School of Medicine, Osaka, Japan **2** Laboratory for Immune Signal, National Institute of Biomedical Innovation

CORRESPONDENCE Atsushi Tanemura, e-mail: tanemura@derma.med.osaka-u.ac.jp
*These authors contributed equally to this work.

KEYWORDS vitiligo/Th17 cell/Th17-related cytokines/melanocyte/interaction with skin-resident cells

PUBLICATION DATA Received 19 July 2011, revised and accepted for publication 30 November 2011, published online 3 December 2011

doi: 10.1111/j.1755-148X.2011.00945.x

Summary

The aim of this study was to determine whether CD4$^+$IL-17A$^+$Th17 cells infiltrate vitiligo skin and to investigate whether the proinflammatory cytokines related to Th17 cell influence melanocyte enzymatic activity and cell fate. An immunohistochemical analysis showed Th17 cell infiltration in 21 of 23 vitiligo skin samples in addition to CD8$^+$ cells on the reticular dermis. An in vitro analysis showed that the expression of MITF and downstream genes was downregulated in melanocytes by treatment with interleukin (IL)-17A, IL-1β, IL-6, and tumor necrosis factor (TNF)-α. Treatment with these cytokines also induced morphological shrinking in melanocytes, resulting in decreased melanin production. In terms of local cytokine network in the skin, IL-17A dramatically induced IL-1β, IL-6, and TNF-α production in skin-resident cells such as keratinocytes and fibroblasts. Our results provide evidence of the influence of a complex Th17 cell-related cytokine environment in local depigmentation in addition to CD8$^+$ cell-mediated melanocyte destruction in autoimmune vitiligo.

Introduction

In the epidermis, the epidermal melanin unit is reliant on the close interaction between a melanocyte and the associated pool of keratinocytes, and several inflammatory cytokines affect melanocyte migration, proliferation, and differentiation. Therefore, the local skin microenvironment generated by the skin-resident cells may be considered a crucial milieu for the normal life and functions of epidermal melanocytes (Chalraborty and Pawelek, 1993).

Vitiligo, a representative depigmented skin disorder associated with melanocyte destruction, affects an estimated 1% of the world's population (Howitz et al., 1977). Although the cellular immunoresponse, mainly of CD8$^+$ cytotoxic T cells, to the melanocyte-specific proteins MART-1, tyrosinase (TYR), and TRPs-1 and -2 has been shown to destroy functional melanocytes in

Significance

Here we show that not only cytotoxic T cells, which have been thought to play a major role in autoimmune vitiligo, but also infiltration of Th17 cells may play a role in vitiligo skin. In fact, we find that in vitro, a network of Th17 cell-related cytokines directly affect melanocyte activity and function, including downregulation of melanin production and shrinkage of melanocytes. These observations may shed light on the functional significance of TH17 cells in autoimmune vitiligo.

autoimmune vitiligo, this does not provide a full explanation for the etiology of vitiligo (Norris et al., 1994; Ogg et al., 1998; Okamoto et al., 1998; Ongenae et al., 2003). In addition to the autoimmune mechanism, recent reports have shown that there is a significant increase in the expression of inflammatory cytokines in affected skin compared with unaffected skin, and several investigators have proposed that the influence of local cytokines may be related to the induction and maintenance of vitiligo (Basak et al., 2009; Moretti et al., 2002, 2009; Ratsep et al., 2008). Although the representative cytokines increased in vitiligo skin have been reported to include interleukin (IL)-2, tumor necrosis factor (TNF)-α, and interferon (IFN)-γ (Caixia et al., 1999), there is no direct evidence of their function in the melanocyte destruction observed in vitiligo.

Upon induction by transforming growth factor (TGF)-b and IL-6, a subset of $CD4^+$ helper T cells develops as Th17 cells (Diveu et al., 2008). IL-17A is a cystine-linked homodimeric proinflammatory cytokine produced by Th17 cells, which form a distinct subset of the $CD4^+$ T-cell lineage. IL-17A stimulates the production of IL-1β, TNF-α, and IL-6 (Kolls and Linden, 2004; Liang et al., 2006). In the past decade, Th17 cells have been identified in autoimmune skin inflammatory disorders such as psoriasis and atopic dermatitis (Asarch et al., 2008; Fitch et al., 2009). A recent study showed a positive correlation between serum IL-17 levels and the extent of the depigmentation patch area in vitiligo, thus suggesting that Th17 cells, rather than regulatory T cells, are involved in vitiligo (Basak et al., 2009). Another study demonstrated elevated IL-17 levels in lesional skin and serum of patients with vitiligo compared with those of controls (Bassiouny and Shaker, 2011). These results indicated the importance of the secreted cytokine environment surrounding vitiliginous melanocytes in terms of vitligo etiology. In the present study, we investigated whether Th17 cells infiltrate vitiligo skin as in cases of psoriasis and whether the proinflammatory cytokines produced by Th17 cells, keratinocytes, and fibroblasts are altered in vitiligous lesions in a series of non-segmental vitiligo patients. The Th17-related cytokines tested included IL-17A and IL-22, in addition to IL-1β and IL-6, which have been reported to inhibit melanocyte activity (Kamaraju et al., 2002; Kholmanskikh et al., 2010).

MITF-M (microphthalmia-associated transcription factor-M) is a master transcription factor regulating melanocyte fate and melanogenic activity; it is distinctly expressed in melanocytes and mast cells (Levy et al., 2006). MITF expression and phosphorylation are important for the regulation of melanogenesis and melanocyte survival because the target genes of MITF encode the apoptosis regulator protein, B-cell lymphoma 2 (Bcl-2), in addition to melanogenic enzymes, tyrosinase, tyrosinase-related protein-1 (TRP-1), and dopachrome tautomerase (DCT), which are indispensable for maintaining melanocyte function (Levy et al., 2006). Because of the reduction in active melanocytes expressing these proteins in the vitiligo epidermis, the dysregulation of MITF expression has to be resolved to effectively treat vitiligo. In addition, the mRNA levels of *MITF* and *BCL2* were decreased in the lesional skin compared with the non-lesional skin of vitiligo patients (Kingo et al., 2008). The expression levels of IL-6 and TNF-α were also significantly higher in the lesional skin, indicating that in vitiligo lesions, there is increased expression of cytokines that are paracrine inhibitors of melanocytes (Moretti et al., 2002, 2009). These cytokines are produced mainly by keratinocytes, so it is possible that these cells may be abnormal in vitiligo. In addition, the expression of cytokines was unchanged in healthy skin compared with non-lesional skin, suggesting that the change observed in vitiligo lesional skin is possibly related to, or contributes to, depigmentation. Therefore, it is conceivable that there is a previously unrecognized mechanism involved in the regulation of the pigmentation-hypopigmentation balance in addition to a cytotoxic effect by $CD8^+$ T cell.

In this study, we examined the direct effect of Th17-related cytokines on MITF expression to determine the effects on the resulting cytokine involvement on the regulation of critical melanocyte behavior. We discuss the significance of Th17 cell infiltration in autoimmune vitiligo skin and propose a functional involvement of Th17 cell-related proinflammatory cytokines in vitiligo.

Results

Vitiligo skin develops in association with Th17 cell infiltration

Approval for this study was obtained from the Institutional Review Board of the Osaka University Hospital. To investigate whether Th17 cells infiltrate vitiligo skin, we performed immunostaining for IL-17A and CD4 using specific antibodies. Th17 cells were defined as the cells expressing both markers after exclusion of gamma delta T cells. Twenty-three vitiligo patients were enrolled in this study (see Table 1 for details) and were divided into 17 generalized, four localized, and two seg-

Table 1. Patients' characteristics and the infiltration status of Th17 cells

Age	27–81			
Gender				
Female	13			
Male	10			
Disease duration (yr)	0.1–26			
Mean	6.2			
	(n)	>50/field	<50/field	Not detected
Th17 cell infiltration				
Generalized type	17	11	6	0
Segmental type	4	2	0	2
Localized type	2	2	0	0
Total	23	15	6	2

mental types. The ages of the enrolled patients ranged from 27 to 81 yr, and the subjects included 13 women and 10 men. As a representative case, we show a 79-yr-old man who had experienced enlarging symmetrical depigmented macules on the whole body including face starting 2 yr previously who was positive for antithyroid antibody in the blood test (Figure 1).

Biopsy specimens were obtained from the leading edge of lesional skin on the left upper arm and were processed for the designated immunostaining. The immunohistochemical analysis revealed significant infiltration of IL-17A$^+$CD4$^+$ cells, that is, Th17 cells, mainly on the reticular dermis and perivascular region (Figure 1A). IL-17A expression was confirmed by RT-PCR using vitiligo tissue RNA. Psoriasis skin, a representative skin disease with Th17 cell infiltration, was loaded as a positive control for RT-PCR (Figure 1A). CD8$^+$ T cells were also observed, mainly below the epidermis, whereas Foxp3$^+$ cells and CD20$^+$ B cells had only faintly infiltrated (Figure 1B). Melan-A positive melanocytes were not observed in the vitiligo epidermis with inflammatory cell infiltration, whereas they were frequently located in the non-lesional skin (Figure 1B lower right panel and Inbox, respectively).

We observed a significant number of Th17 cells in 21 of 23 of the patient skin samples, and more than 50 double-positive cells per high power field were observed in 15 patients, while there was sparse infiltration in normal skin. Th17 cells were not detected in the two cases of localized type. Psoriatic skin was used as a positive control for this staining and showed the involvement as dense infiltration through the epidermis and upper dermis of pathogenic inflammatory cells whose localization was different from that in vitiligo (Figure 1C). Although we suspected that early onset and generalized type vitiligo had more opportu-

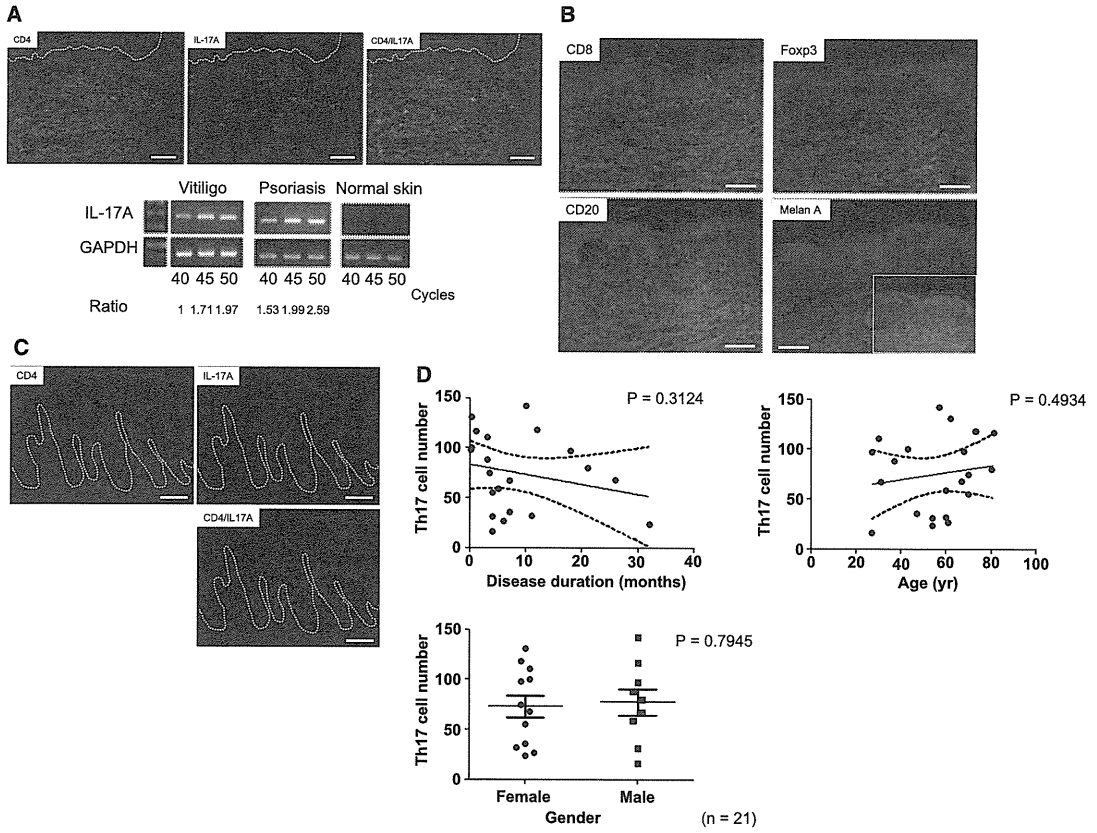

Figure 1. Photographic features of a representative generalized vitiligo patient and the immunohistochemical analysis for infiltrating cells in vitiligo skin. Multiple- and symmetrical-depigmented macules were present on the face and upper arm. A spindle-shaped skin specimen was obtained from the leading edge of an upper arm lesion. Immunostaining for CD4 and IL-17A in the vitiligo skin lesion indicated the significant infiltration of Th17 cells (yellow) positive for both CD4 (green) and IL-17A (red) mainly on reticular dermis and perivascular region. RT-PCR confirmed the same level of IL-17A expression in the vitiligo skin as in psoriasis skin (A). CD8-positive cytotoxic T lymphocytes (CTLs) (red, upper left) infiltrated the upper dermis and epidermis, whereas Foxp3 and CD20 positive cells (upper right and lower left) were only faintly detected. Melan-A-positive cells, highly differentiated melanocytes, were present in the normal region (lower right, small window), whereas they were absent in the vitiligo epidermis (lower right) (B). Psoriatic skin showed Th17 cell infiltration in the papillary dermis in addition to the epidermis (C). All images are original magnification ×40 for vitiligo and ×100 for psoriatic skin. The white bar indicates 100 μm. (D) The mean Th17 cell number present in vitiligo skin was counted on three independent fields, and the correlation with disease parameters such as disease duration, age, and gender was evaluated (n = 16).

nity to be infiltrated by Th17 cells, there was no significant correlation between the number of infiltrating Th17 cells and the clinical type, or with disease parameters such as disease duration, age, or gender in 21 patients with Th17 cell infiltration (Figure 1E).

Proinflammatory cytokines associated with Th17 cells influence in melanin activity

Because a significant number of Th17 cells were found in most of the vitiligo skin samples examined in this study, we hypothesized that there was a possible role for Th17 cell-related cytokines in melanocyte activity. Previous reports have shown that several cytokines downregulated tyrosinase activity through the activation of designated intracellular signaling pathways (Englaro et al., 1999; Kamaraju et al., 2002; Kholmanskikh et al., 2010). We therefore decided to examine the effects of IL-1β, IL-6, IL-17A, and IL-22, which are important cytokines induced by Th17 cell differentiation and maintenance, on melanocyte development and activity. MITF, a pivotal transcription factor related to melanocyte function and survival, expression and translocation was at first examined by immunocytochemistry (Figure 2A, C). Whereas there was apparent translocation of the MITF protein to the nucleus in untreated cultured melanocytes (Figure 2A), the MITF expression was decreased in the nucleus of the melanocytes treated with 10 ng/ml of IL-1β or IL-17A (Figure 2B, C), suggesting that there was a reduction in MITF-related signaling in melanocytes following cytokine treatment. In contrast, IL-22 treatment had no effect on melanocytes (data not shown), so we decided not to include IL-22 in the further experiments.

Next, we examined the expression of cytokine receptors by RT-PCR to confirm the ligand-to-receptor correspondence in melanocytes. Cultured human melanocytes were found to express IL-1R1, IL-6R, and IL-17RA without the addition of cytokines, whereas treatment with 10 ng/ml of their corresponding

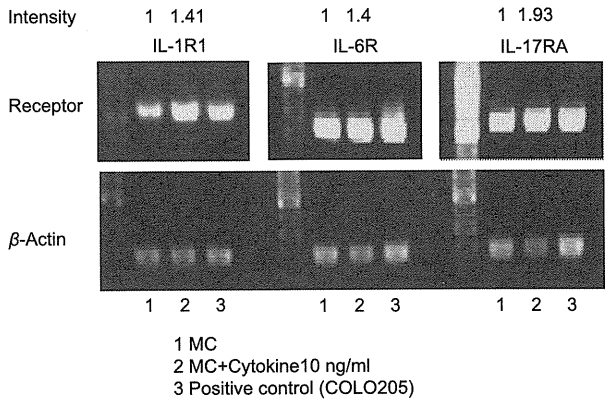

Figure 3. The expression of cytokine receptors in human melanocytes. IL-1R1, IL-6R, and IL-17RA mRNA were expressed in human melanocytes and were upregulated following treatment with their corresponding cytokines. COLO205 cells (colon cancer cell line) were used as a positive control. β-actin was used as a housekeeping gene.

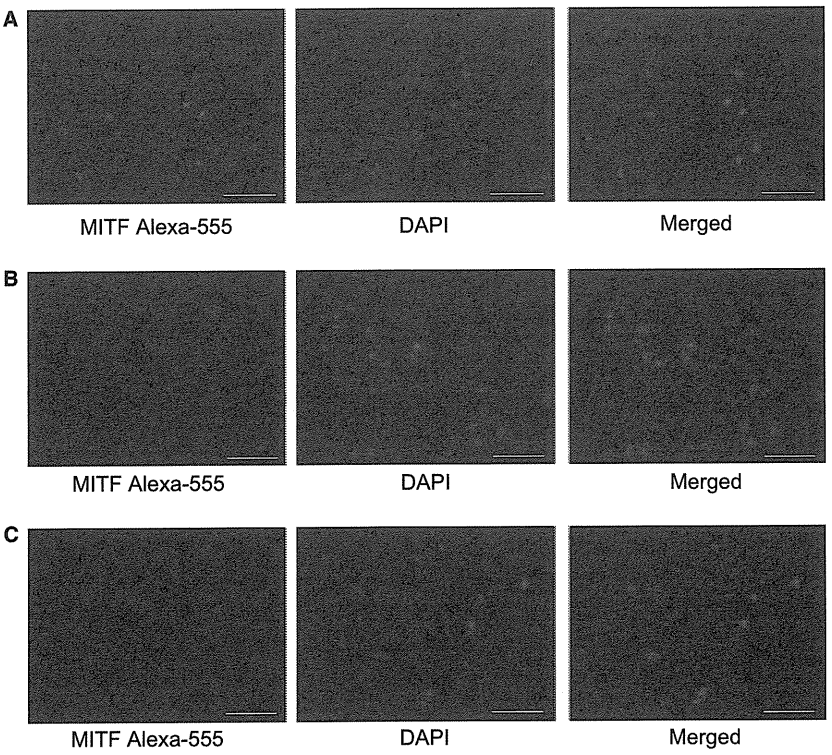

Figure 2. Immunocytochemical staining for MITF in human melanocytes. MITF was expressed mainly in the nuclei of untreated cells (A). In contrast, MITF expression was decreased after treatment with recombinant IL-1β (B) and IL-17A (C). The white bar indicates 50 μm.

cytokines increased receptor expression (Figure 3). COLO205 cells, the human colon cancer cell line expressing these receptors endogenously, were loaded in parallel with cultured melanocytes as a positive control.

To investigate the direct effects of Th17 cell-related cytokines on melanocytes in vitro, we examined the mRNA expression of melanogenic and melanocyte survival molecules after treatment of human melanocytes with recombinant human cytokines (Figure 4). The expression of *MITF*, which encodes a master transcription factor that regulates melanocyte function; of *TYR*, *TRP-1*, and *DCT*, which encode enzymes involved in melanin synthesis; and of *BCL2*, which encodes an anti-apoptotic protein, was measured by quantitative PCR. MITF expression was found to be significantly decreased in a dose-dependent manner after treatment with IL-1β, IL-6, and TNF-α (Figure 4A). The *MITF* transcription level decreased to <50% after treatment with 1 ng/ml of TNF-α. MITF was downregulated by 10 ng/ml IL-17A. In terms of the expression of its downstream enzymes, IL-1β significantly downregulated the genes, but only at a concentration of 10 ng/ml, whereas basic FGF upregulated their expression. IL-6 downregulated *TYRP1* and *DCT*, but there was no significant decrease in *TYR*. A 10 ng/ml concentration of IL-17A was needed to induce their significant downregulation. On the other hand, TNF-α significantly suppressed the expression of

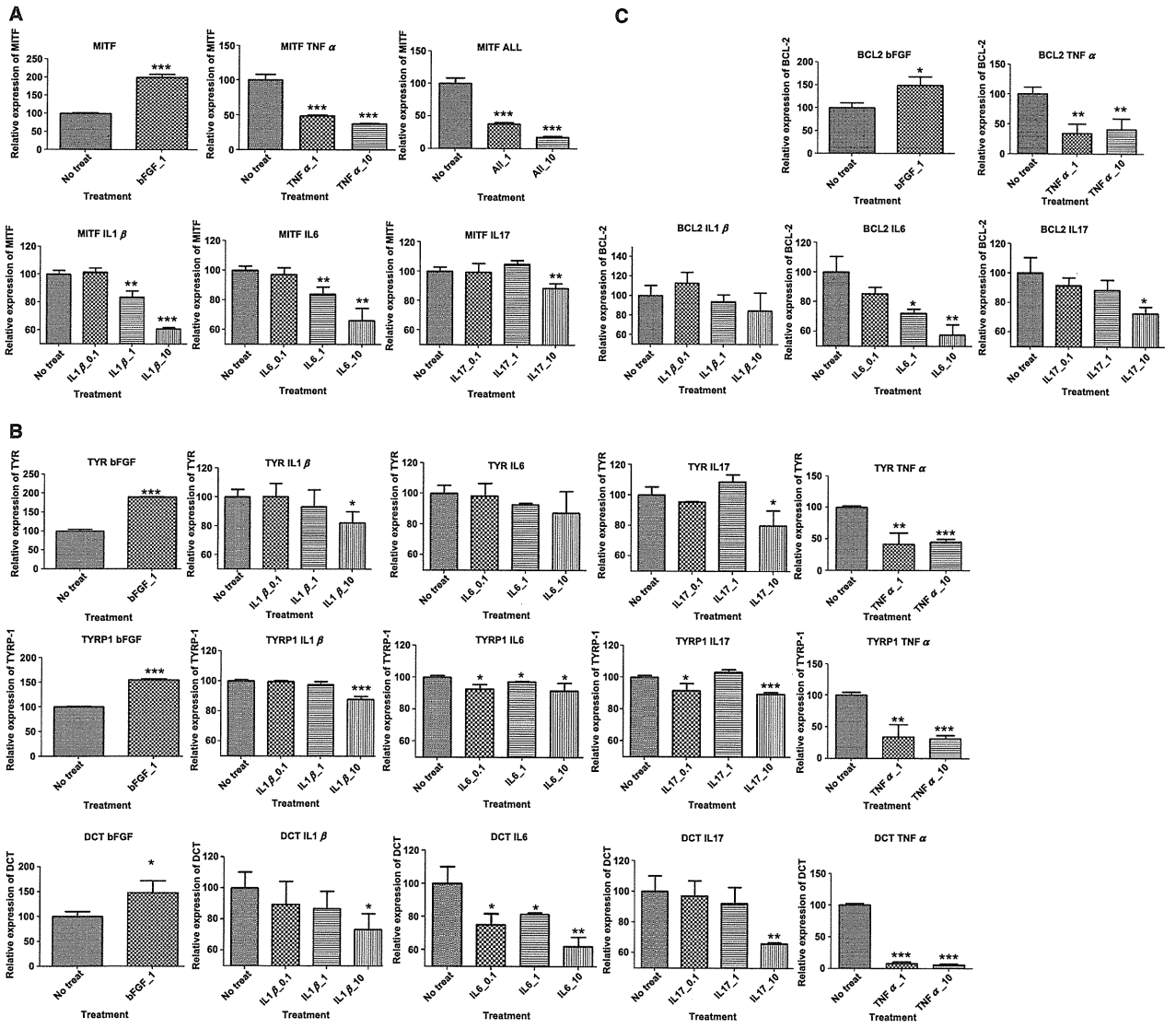

Figure 4. The quantitative analysis of the mRNA expression of MITF and genes encoding melanogenic enzymes. Human melanocytes were incubated with recombinant cytokines for 4 h at concentrations of 0.1, 1, or 10 ng/ml in the culture medium. The mRNA expression levels of MITF (A), genes encoding melanogenic enzymes (B), and B-cell lymphoma 2 (Bcl-2) (C) were measured by qRT-PCR. *P < 0.05; **P < 0.01; ***P < 0.001 compared with the expression level in untreated control cells.